

PERFORMANCE REQUIREMENTS OF HIGH
QUALITY FLEXIBLE PAVEMENTS

by

Douglas Bynum, Jr.

and

R. N. Traxler

Research Report No. 127-1
Research Study No. 2-8-69-127

Sponsored by

The Texas Highway Department
In Cooperation with the
U. S. Department of Transportation
Federal Highway Administration
Bureau of Public Roads

August 1969

TEXAS TRANSPORTATION INSTITUTE
Texas A&M University
College Station, Texas 77843

ABSTRACT

This study involved the development of performance requirements to alleviate thermal distress in a high quality surface course for flexible pavement. The four requirements determined were for (1) long term or thermal equilibrium, normal strain or stress, (2) short term or transient thermal stress, (3) shear strength and (4) peel strength of the pavement-foundation interface. The shear lag in the asphaltic concrete was found to increase with increasing thickness of lifts. A time-temperature dependent modulus was used to compute stresses so the results were thermoviscoelastic requirements. Use of the results will lead to conservative design from the standpoint of maintaining the structural integrity of the pavement.

TABLE OF CONTENTS

	PAGE
ABSTRACT	ii
TABLE OF CONTENTS.	iii
LIST OF FIGURES.	v
 CHAPTER	
I Introduction	1
1.1 Objectives of Overall Study	1
1.2 Scope of the Reported Research.	2
1.3 Related Continuing Research	4
II Background	6
2.1 Summary	6
2.2 General	7
2.3 Factors Affecting Pavement Performance	10
2.4 Thermal Environment	16
2.5 Mechanically Induced Distress	25
III The Energy Method of Applied Mechanics	37
IV An Approximate Energy Solution for Thermal Distress	41
V Thermal Distress with Variable Temperature	51
5.1 Distribution of Normal Stress and Strain in the Asphaltic Concrete Layer	51
5.2 Shear Distress at the Pavement- Foundation Interface.	56
5.3 Peel Distress	58
VI Discussion of Results.	64
6.1 General	64
6.2 Equilibrium Thermal Distress.	65
6.3 Transient Thermal Distress.	68
6.4 Shear State at the Pavement- Foundation Interface.	69
6.5 Debond by Peel Mechanism.	70
6.6 Implications of the Results	71

TABLE OF CONTENTS (CONT'D.)

CHAPTER	PAGE
VII Conclusions and Recommendations	73
7.1 Conclusions.	73
7.2 Recommendations.	74
NOMENCLATURE.	77
REFERENCES.	80

The opinions, findings, and conclusions expressed in this publication are those of the authors and not necessarily those of the Bureau of Public Roads.

LIST OF FIGURES

FIGURE		PAGE
1	Determination of Performance Requirements	3
2	Layers in Flexible Pavement	9
3a	Qualitative Representation of Factors Affecting Flexible Pavement Performance	11
3b	Qualitative Representation of Factors Affecting Flexible Pavement Performance	12
3c	Qualitative Representation of Factors Affecting Flexible Pavement Performance	13
4	Classification of the Approaches to Flexible Pavement Design	14
5	Factors Related to Transverse Crack Development	17
6	Temperatures During Application of Hot Plant Mix Stabilized Base. Single Lift 12-In. Compacted Thickness	20
7	Cooling Temperature During Application of Hot Plant Mix Stabilized Base. Single Lift 12-In. Compacted Thickness	21
8	Cooling Curves--Set 2, Station IV-1	22
9	Hourly Temperatures in June	23
10	Average Annual Frost Penetration, in Inches	24
11	Schematic of Strain Distribution Single and Dual Wheel Loading	26
12	Strain Variation on Surface of Pavement for Single Axle Truck--Creep Speed--(Approximately 4 mph)	27
13	Strain Variation on Surface of Pavement for Single Axle Truck--20 mph Velocity	28
14	Influence of Stiffness Ratio	29

LIST OF FIGURES (CONT'D.)

FIGURE		PAGE
15a	Cross Section of Laboratory Highway Test Track Showing General Scheme of Installation	31
15b	Pressure Distribution Under 500-Pound Load as Affected by Slab Thickness, Temperature at 70°F	31
16	Deflection Contours and Profiles 18-Kip Single Axle Load--WASHO Road Test	32
17	Deflection Contours and Profiles 40-Kip Tandem Axle Load--WASHO Road Test	33
18	Effect of Temperature on Deflection	35
19	Deflection Patterns	36
20	Schematic of States of Thermal Distress	42
21	Master Modulus and Compliance	52
22	Master Shift Factors	53
23	Schematic of Non-Uniform Temperature Distribution in the Flexible Pavement	55
24	Progression of Peel Mechanism	59
25	Separation Due to Foundation Shift (Frontage Road near New Braunfels	61

CHAPTER I

INTRODUCTION

1.1 Objectives of Overall Study

High grade flexible pavement surfacings are usually designed for a 20-year life; however, the actual life is sometimes less than the design life due to incalculable variables. Damage to the flexible pavement is primarily a result of distress due to cyclic thermal strains resulting from ambient temperature variations, fatigue due to traffic loads, a result of foundation shifts, aging (hardening) of bituminous binders, and instability (shoving, rutting).

This reported work is a part of a continuing research study at the Texas Transportation Institute, sponsored by the Texas Highway Department and the Bureau of Public Roads. The objectives of the overall study are to:

1. Determine the performance requirements of the material needed to serve as the cohesive-adhesive waterproof binder for a first-class, long-life flexible pavement surface course,
2. Develop control tests for use in a specification for a material that will meet the performance requirements in objective one, and,

The citations on the following pages follow the style of the Proceedings of the Association of Asphalt Paving Technologists.

3. Concurrently with objective number two, search for a cohesive material that will meet the requirements of objective number one.

1.2 Scope of the Reported Research

Some of the considerations necessary for a successful determination of the performance requirements of a high quality wearing course on a flexible pavement are given in Fig. 1. Because the conditions of thermal distress have received the least attention in the past, work considered in this report is directed mainly toward the requirements necessary to satisfy the thermal environment.

More specifically, the particular problems covered here are the development of the solutions for long term strain distribution in the pavement due to variable thermal constraint, short term strain distribution due to variable temperature of the pavement, required shear strength of the pavement-foundation interface, and the required peel strength of the pavement. Calculations using the developed solutions are given.

Osborn (1) has suggested that the problem solving process involves two factors: judgment or the ability to think logically, and imagination or the ability to think creatively. The creative problem solving processes include fact-finding (defining the problem and collecting data), idea finding (thinking out many ideas), and solution finding (evaluating and deciding on which ideas to use). In regard to fact-finding, it might be noted that nothing could be

found in the literature concerning the use of peel strength as a performance criterion for use in highway design.

1.3 Related Continuing Research

To better understand the approach to the overall research objective, and how the work reported below fits into the project objective, other tasks being concurrently pursued will now be mentioned.

1. The available constitutive equations and conversion formulas used in linear viscoelasticity are being reviewed. This should be useful since the viscoelastic nature of flexible pavements is ordinarily neglected in highway design work, and further, the use of conversion formulas can greatly reduce the effort required for tests to determine material properties.

2. Some of the most sophisticated finite element digital computer routines currently used in the aerospace industry have been obtained. The modification of these routines for thermoviscoelastic analysis as well as for the analysis of distress due to mechanical loads is being considered.

3. The material property tests currently being used by the solid propellant rocket motor industry are being reviewed for application in highway design. A total factorial design of material property tests using these new test methods and a standardized aggregate is being planned. Tests in a partial replicate design will be performed using real aggregates for comparative purposes.

4. The use of gel permeation chromatography for quality specification of asphalts and assessment of accumulative damage by aging has been considered. The results of preliminary studies indicate that this is a feasible approach.

CHAPTER I I

BACKGROUND

2.1 Summary

From the review of a voluminous amount of research data (approximately 650 technical papers and reports), several points of interest emerged, which are summarized as follows:

a. The present state of the art in pavement design is to a considerable extent dependent on experience and empirical data. A truly scientific approach has not been developed because of the extremely complex nature of the problem.

b. A scientific technology has evolved in the aerospace and other industries (e.g. rubber, etc.) in recent years and has been accelerated in the solid propellant missile industry, in particular. This was necessitated by the very rigid demands for effectiveness and reliability. Because of the similarities between the material behavior and the structural state of solid propellant motors and flexible pavements, an exciting potential exists for transferring rocket motor technology to pavement design without excruciating financial strain.

c. Previous researchers apparently have developed large amounts of data obtained for specific conditions without giving full consideration to all of the interactions between the variables involved. It would therefore seem appropriate to consider a reference

set of material property data using a standard mixture for comparison with real mixtures. Knowing the ratios of material property data with respect to a standard would enable a quantitative comparison of the results obtained in various laboratories to be made.

d. From the short-term economical standpoint, asphalts are by far the best binder candidates known, but from the performance standpoint bitumens may be inferior because of their delayed effects, e.g. embrittlement with time, oxidation, etc. Viewing high quality flexible pavements from the long-term economical point of view, asphalts may be poor binder candidates because of excessive maintenance costs. By the use of (a) new design innovations, (b) certain composite aggregates in the base course, and (c) modified asphalt binders or new binder materials in the wearing course, flexible pavements could undoubtedly be constructed more economically for short-term and long-term service with an improved structural integrity of the pavement.

2.2 General

Asphalt concrete pavement usually consists of about 6% asphalt binder by weight, a stone-aggregate filler, and air voids which usually vary between 3 and 6% of the total mixture volume (2) depending on the design. As a matter of interest, the current annual production of asphalt in the U. S. is about 25 million tons, of which about 18 million tons are used in highway and related construction. The remainder is used for various purposes such as lining

reservoirs, manufacture of roofing, and specialty products.

Recent figures from the U. S. Bureau of Public Roads (3) show that in 1965 the road and street mileage in the United States amounted to 3,689,666 total miles, including 1,339,456 miles of asphaltic concrete, 115,144 miles of portland cement concrete, 1,321,457 miles of gravel roads, and 913,609 miles of earth roads. Approximately 45,000 miles per year of paved roads and streets are added to the existing network of 1,454,600 miles of pavement. Since each new mile of pavement is accompanied by the consumption of about 50,000 additional gallons of motor fuel per year, then at 10 cents tax per gallon, every new mile of paved road generates approximately \$5,000 per year.

The nomenclature used here for the layers in flexible pavement is given in Fig. 2. The thickness of the subbase, if this layer is used in the construction, varies between 6 inches and about 2 feet and the base course usually has similar dimensions. The surface treatment or prime coat usually consists of the application of about 0.3 gallons of hot asphalt per square yard, whereas about 0.1 gallons of hot asphalt per square yard is applied in the tack coat. The seal coat, usually applied from two to five years after construction and whenever needed thereafter, consists of between 0.2 and 0.4 gallons of hot asphalt per square yard followed by a cover of fine aggregate.

Hills and Brien (4) have given an excellent approximate procedure for calculating differential temperature ranges to cause fracture in asphaltic pavement. The limitations of the procedure

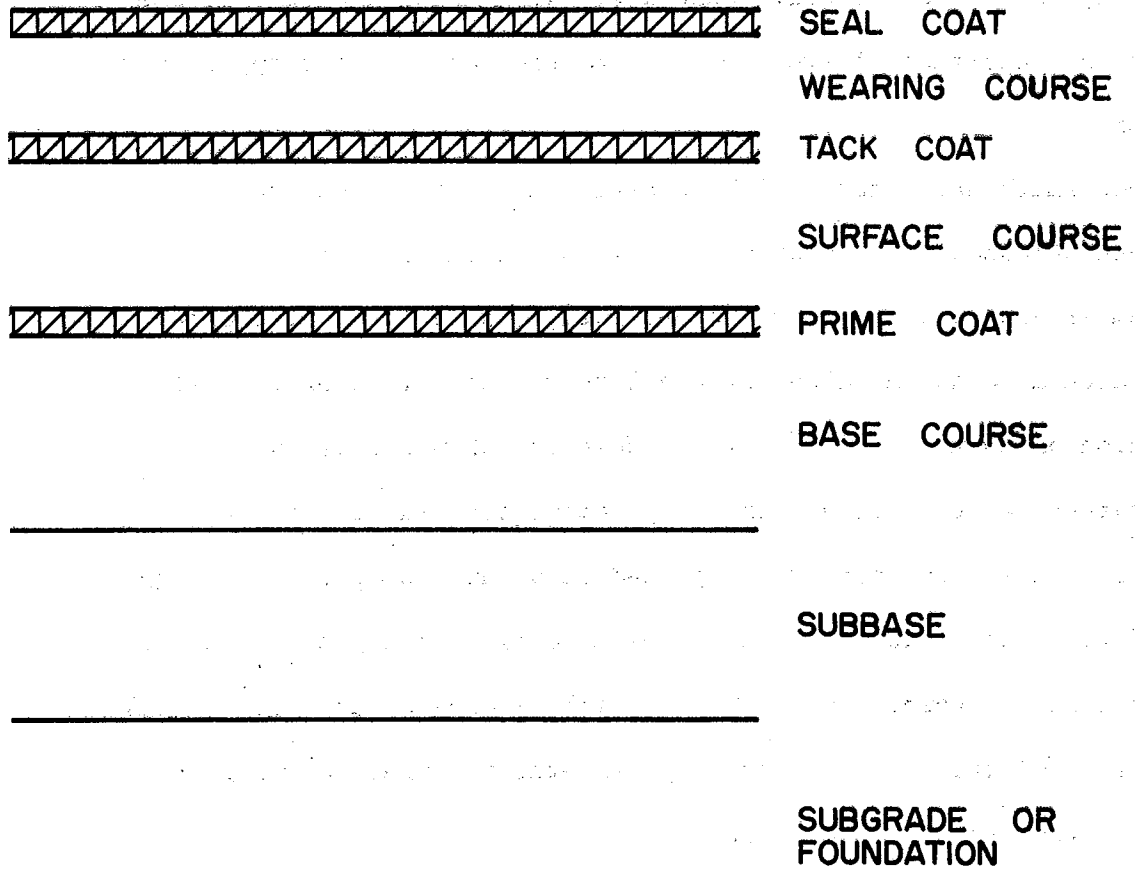


Fig. 2. Layers in Flexible Pavement.

are that elastic constants instead of viscoelastic constants are used for the pavement and the boundary conditions are considered as end fixity on the plate and beam analogies. This means that the pavement-foundation interface distress was not considered in their approximate analysis.

Monismith and Secors (5) have estimated that the surface pavement stresses reach peak values of 40 psi and 140 psi daily in the summer and in the winter, respectively, using particular creep compliance data and a value for the linear coefficient of thermal expansion of 13×10^{-6} in./in./°F. However, when the daily temperatures at the surface of the pavement oscillated between 0 and -40°F, the estimated stress peaked at about 3300 psi, which is considerably above the maximum ultimate tensile strength of asphalt concrete at any temperature. This vividly indicates the exponentially increasing distress with decreasing temperature, i.e. as the glass point of the asphalt is approached.

2.3 Factors Affecting Pavement Performance

Hutchinson and Haas (6) have listed some of the factors affecting flexible pavement performance (Fig. 3) and they indicated that thermal stresses are a major contributing cause of cracking. They also presented an excellent summary (Fig. 4) of design methods from judgment in 1900 to current statistical evaluations of field tests, such as the AASHO tests.

11

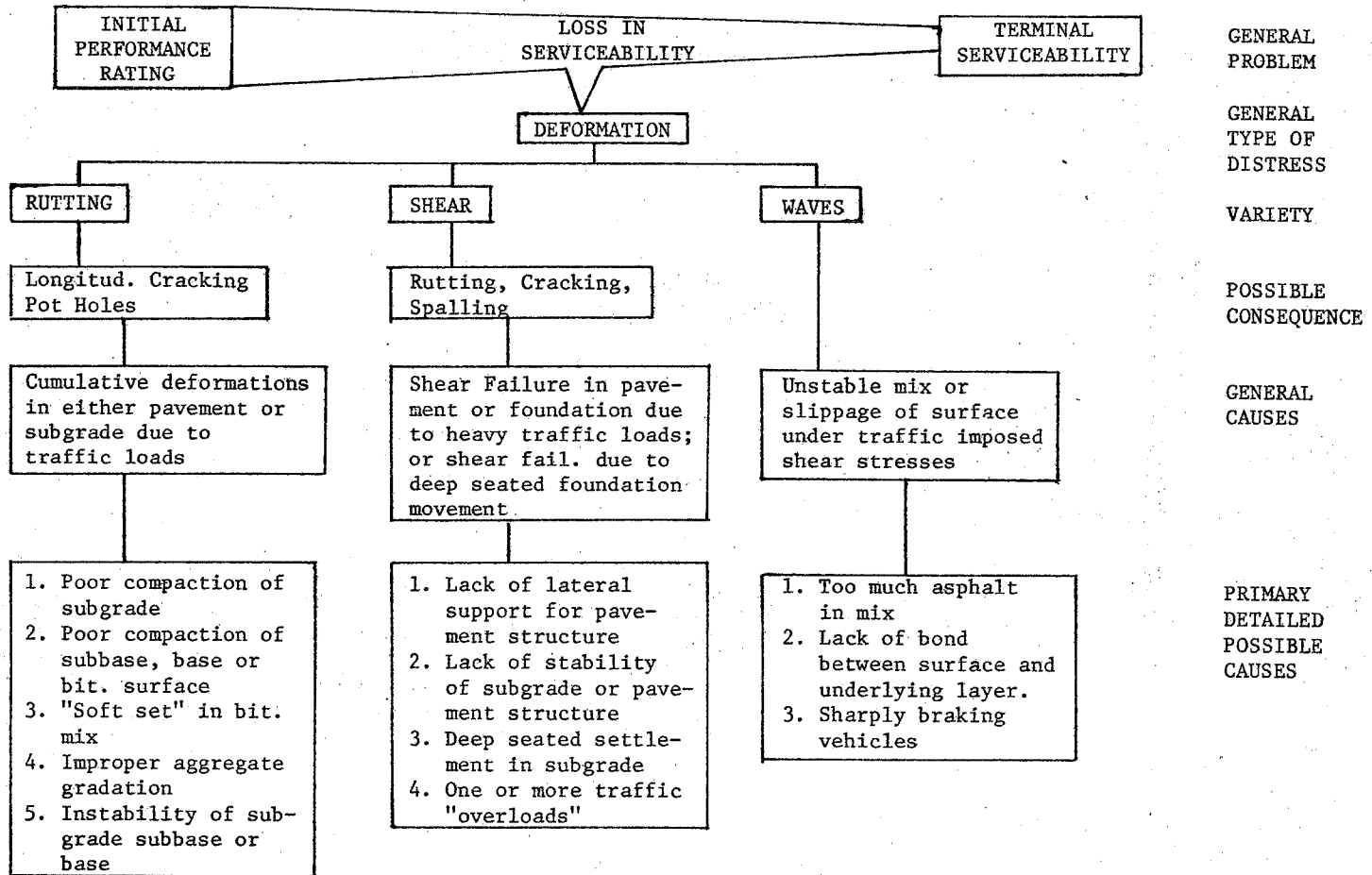
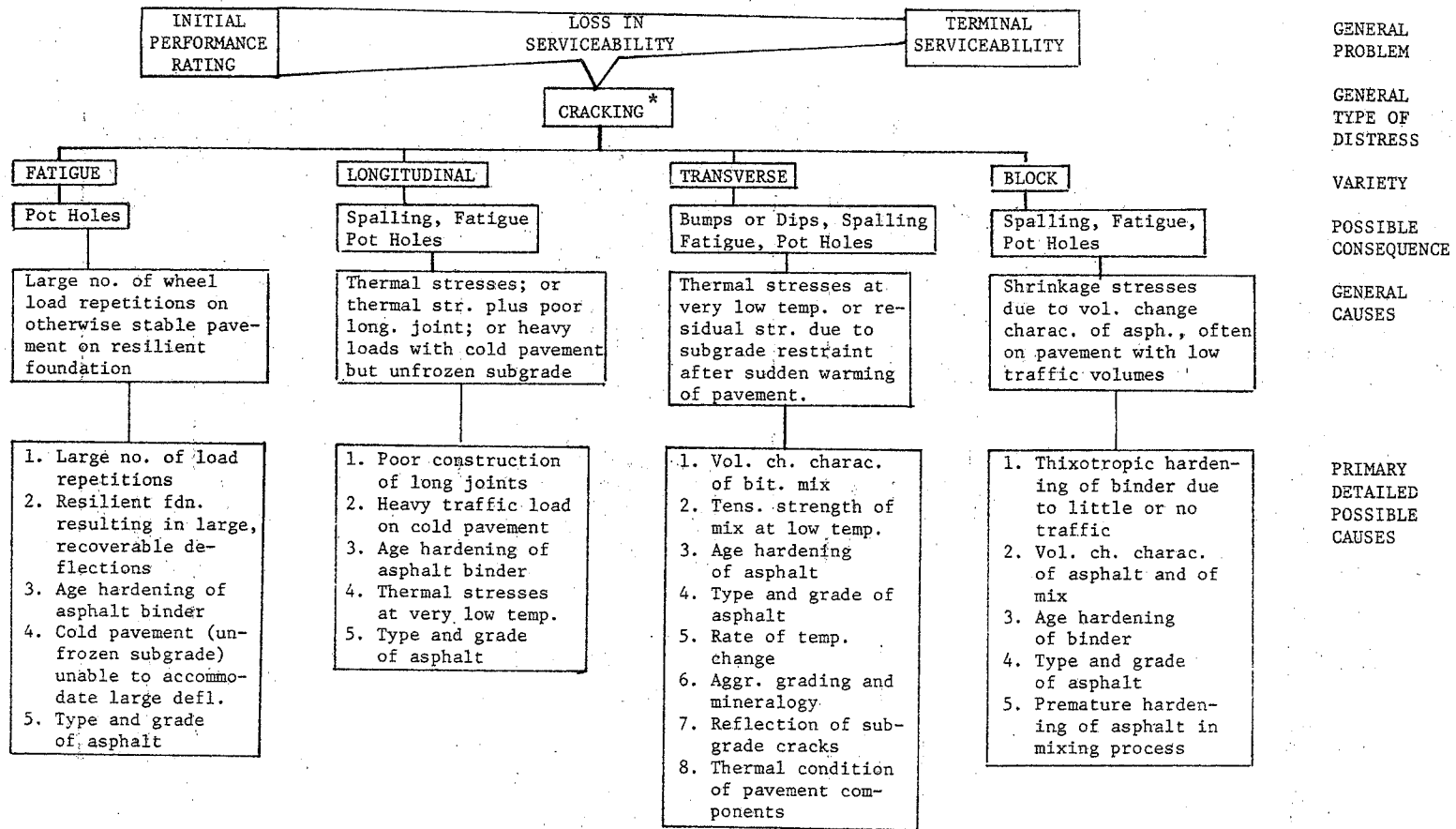


Fig. 3a. Qualitative Representation of Factors Affecting Flexible Pavement Performance (6).



* Does not include reflection cracking in bituminous overlays.

Fig. 3b. Qualitative Representation of Factors Affecting Flexible Pavement Performance (6).

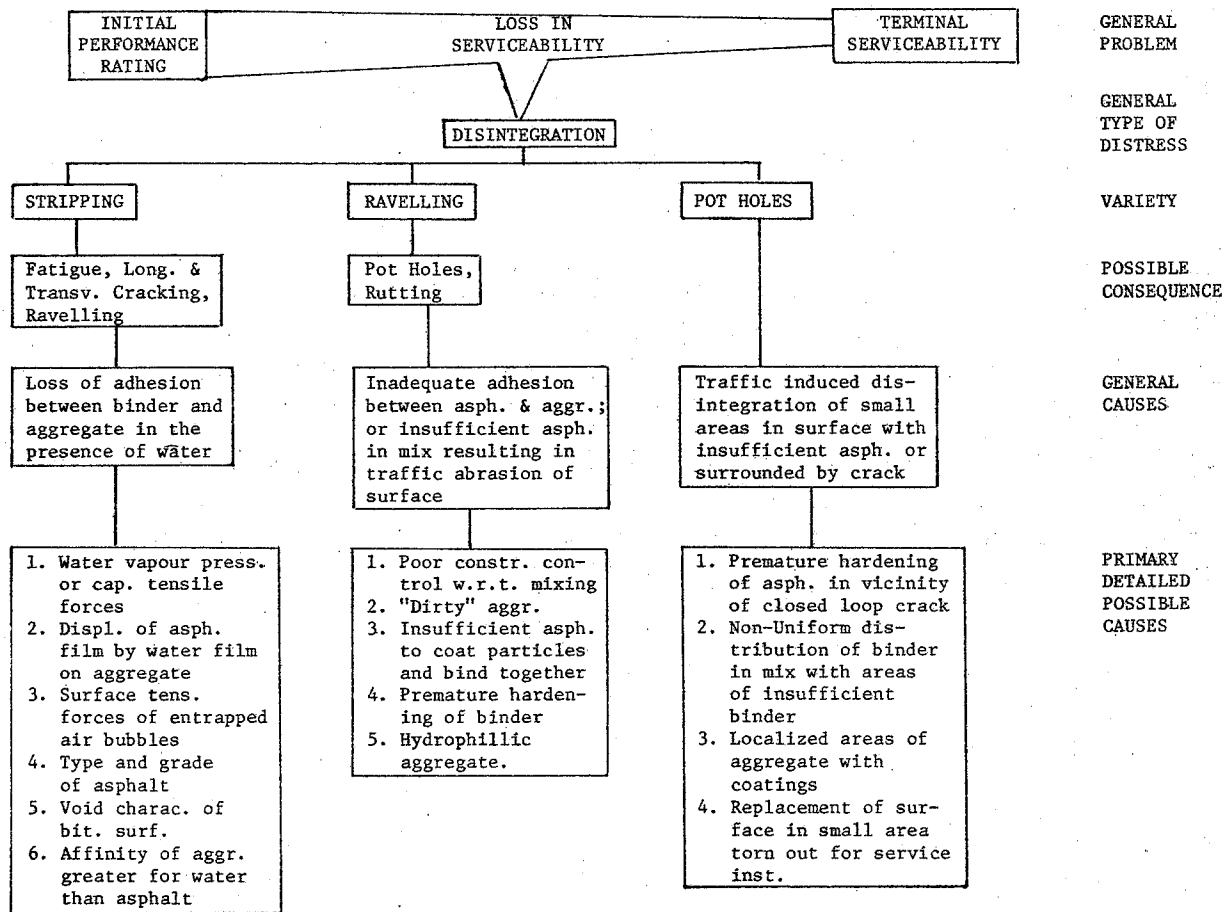


Fig. 3c. Qualitative Representation of Factors Affecting Flexible Pavement Performance (6).

METHODS	FEATURES	LIMITATIONS
A <u>METHODS BASED ON "JUDGEMENT"</u> Examples: Most Can. & U.S. Urban Centers, Ont. Dept. of Hwys.	Attempt to prevent failure. Simple and quick in application. Negligible design costs.	(1) No provisions in method for economic comparisons of pavement type alternatives (A,B,C,D,E,F,G).
B <u>METHODS BASED ON SIMPLE STRENGTH TESTS</u> Examples: CBR or Modified CBR Method, U.S. Corps of Engr., Wyoming.	Attempt to prevent failure. Simple equipment & proceedings for measuring subgrade and base properties. Empirical correlation with pavement thickness.	(2) Weak, subjective link between design and performance evaluation (A,B,C,D,E,F). (3) Failure to recognize effect of layers (A,B,C).
C <u>METHODS BASED ON SOIL FORMULA</u> Examples: Group Index Methods, Can. Fed. D.P.W., U.S. F.A.A. Method.	Attempt to prevent failure. Simple soil classification tests to assign mean expected strength values to subgrade. Empirical link with pavement thickness.	(4) Environmental effects accounted for in only a very subjective manner (A,B,C,D,E,F). (5) Failure to account for effect of repeated loads on pavement deterioration (A,B,C,D,F).
D <u>METHODS BASED ON TRIAXIAL TEST</u> Examples: Kansas Method, Texas Method, California Method.	Attempt to prevent failure. Test values can be used in stability analysis of pavement components and subgrade.	(6) Variations in construction quality not adequately accounted for (A,B,C,D,E,F). (7) Failure to recognize progressive nature of pavement deterioration by considering only failure or non-failure condition (A,B,C,D,E,F).
E <u>METHODS BASED ON PLATE BEARING TEST</u> Examples: U.S. Navy Method, Can. D.O.T. Method.	Attempt to prevent failure by limiting deflection. Full-scale testing of subgrade and pavement structure reaction to load.	(8) No distinction between static or moving nature of loads (A,B,C,D).
F <u>METHODS BASED ON STRUCTURAL ANALYSIS OF LAYERED SYSTEMS</u> Examples: Burmister's Method Shell 3-Layer Method.	Attempt to control or avoid failure mechanisms. Objective analysis to predict stresses and strains at any point in pavement or subgrade.	(9) Inadequate recognition of seasonal strength variation of subgrades (A,B,C,D,F).
G <u>METHODS BASED ON STATISTICAL EVALUATION OF PAVEMENT PERFORMANCE</u> Examples: Design Eqn. from AASHTO Test, CGRA Design Guide.	Attempt to measure performance v. age relations and to control failure age by limiting deflections. Full-scale testing and evaluation.	(10) Simulation of in-service material behaviour not adequately evaluated in laboratory testing (A,B,C,D,F).

1900 1910 1920 1930 1940 1950 1960 1967

Fig. 4. Classification of the Approaches to Flexible Pavement Design (6).

Prior to the Symposium, "Non-Traffic Load Associated Cracking of Asphalt Pavements," which appeared in the 1966 AAPT Proceedings, very little attention had been devoted to the analysis of thermal stress, while hundreds of published papers were readily available that described the response to wheel loads, determined from laboratory and field tests and theoretical procedures. In the few instances where thermal distress was considered, the elastic approach was usually used, as outlined by Hills and Brien (4). The elastic approach is probably best for preliminary design, but the thermo-viscoelastic approach is the natural procedure to use in final designs.

It is not clear how pavement behavior can be adequately described in terms of elastic constants, which has been the past practice. The recent work of Schweyer and Busot (7), and George (8) demonstrates the necessity for considering the behavioral characteristics in terms of rheological constants. The Chou-Larew investigations (9) show that while the maximum stress due to a wheel load occurs when the wheel is directly on a station, the displacements continue to increase for awhile as the load moves away from the station.

The complexities of material properties, environmental conditions, and type of design make the analysis of crack development quite difficult. Anderson, Shields, and Dacyszyn (10) show a flow chart of the various factors and considerations related to crack

development (Fig. 5). Zube (11) reports that the most commonly accepted causes of cracks appearing in asphalt pavements are:

- a. Shrinkage caused by temperature variations in the asphalt binder.
- b. Reflection cracks caused by transmission of cracks in the base.
- c. Cracks caused by expansion and contraction of the foundation.
- d. Cracks due to embrittlement of the binder (oxidation, volatilization, etc.).
- e. High shear susceptibility of the binder resulting in contraction cracks.

2.4 Thermal Environment

Dodd (12) has summarized the latest revision of Army Regulation 705-15, Operation of Material under Extreme Conditions of Environment, in the form of climatic categories. The daily variation of **temperature** in category 5 is approximately a sine wave with a minimum of 70°F at 0500 hours and a maximum of 110°F at 1400 hours. The relative humidity also approximates a sine wave, but with about 10 hours phase lag, i.e. a minimum of 20% at 1300 hours and a maximum of 85% at 0400 hours.

In the WASHO Road Test (13) the distribution of daily air temperature vs time was a sinusoidal mode with the peak occurring about

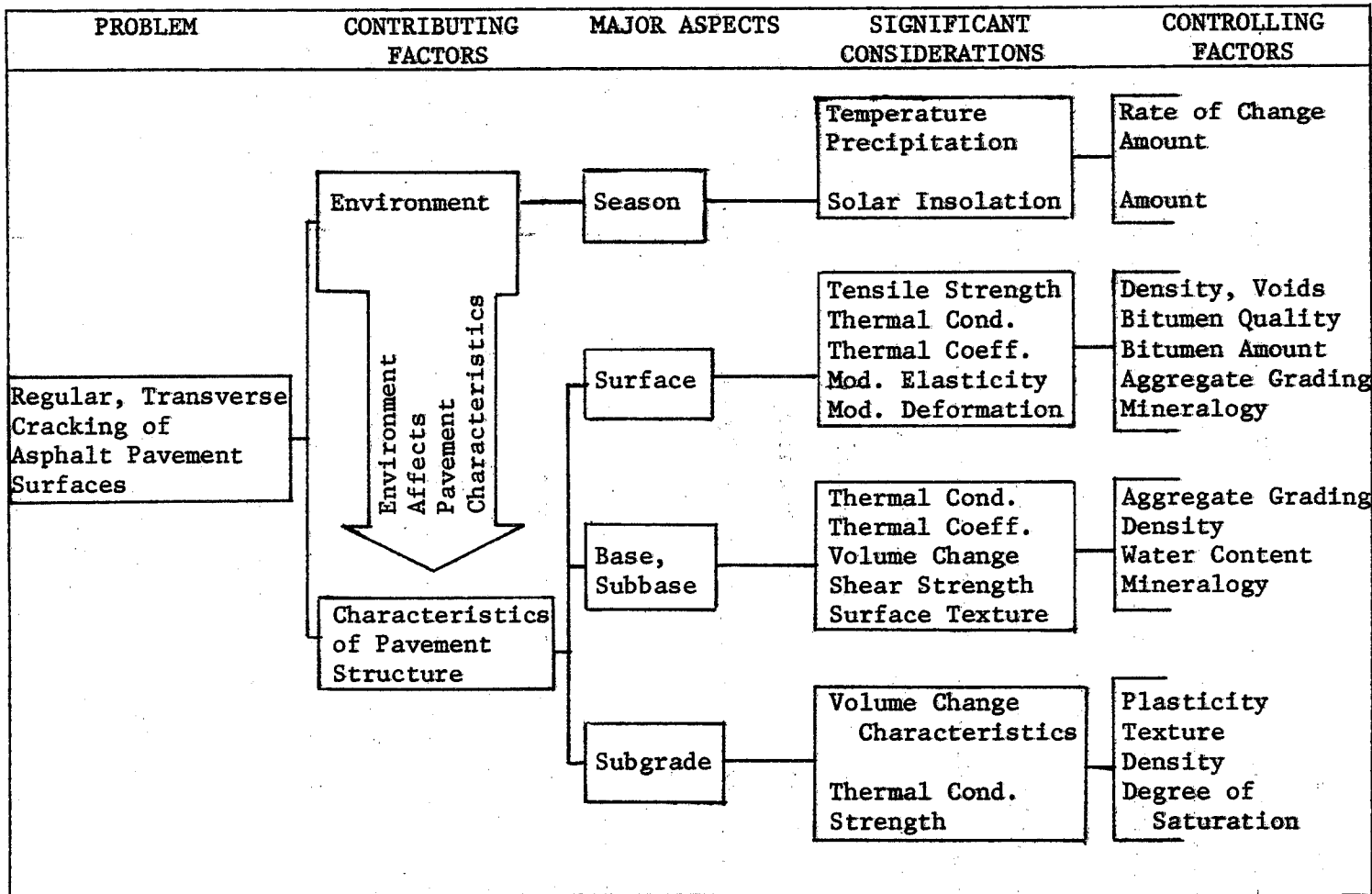


Fig. 5. Factors Related to Transverse Crack Development (10).

1500 hours. Typical extremes and ranges of temperature at the pavement surface were

124-65=60°F/day in July; 37-22=15°F/day in January.

A heat transfer analysis was performed by Monismith, Secor, and Secor (5) to find the temperature at depths in the pavement of 4 in. and 8 in. when the temperature of the pavement surface varied in a sine cycle over one day with the extremes at 0 and -40°F. The temperature lag of course increases as the depth increases, to wit, if at 12 hours from the beginning of the cycle the surface temperature is an extreme of -40°F, then the pavement at a 4 in. depth reaches an extremum of -6°F in 19 hours. Summarily, the maximum daily temperature differences were 32.5°F and 36.5°F for 4 in. and 8 in. depths, respectively.

During his study of the migration of moisture in clay, Moore (14) collected some significant temperature data. It was determined that in College Station, Texas, the average daily change in temperature at the pavement edge was about 20°F, the average change through the pavement was about 10°F, and the maximum seasonal variation of the pavement surface at the centerline of the street was from about 55°F in the first part of January to about 110°F in the latter part of July.

The most comprehensive data found in the literature concerning pavement temperature distribution during and immediately after the application of the pavement to the roadbed was in the work by Beagle (15). He determined the time-temperature-depth topology during and

after the construction of 12-, 15-, and 18-in. lifts (Figs. 6 and 7). Styrafoam was stapled to the subgrade before laying the mix, which because of this insulation resulted in a much higher compaction at the bottom than would have been attainable otherwise. While not mentioned in Beagle's paper, the styrafoam probably acted as a thermal floater for preventing cracks at the pavement-foundation.

Bright, Steed, Steele, and Justice (16) obtained cool down temperature data during the application of a wearing course at mix temperatures of 225 and 345°F (Fig. 8). In their first set of experiments the structure consisted of 4.5-in. thick bituminous concrete course over a gravel base, which was covered with a 1.5-in. binder course followed by a 1-in. surface course. The structure was the same in their second set of experiments except that the 4.5-in. thick bituminous concrete had been laid over an old 5-in. thick concrete pavement.

Kallas (17) determined the continuous temperature distribution at various depths in a 12-in. lift in Maryland. In the month of June the surface temperature varied daily between about 76 and 138°F whereas the temperature at the 12-in. depth ranged from 85 to 95°F (Fig. 9).

Johnson (18) has provided a map of the U. S. showing the annual depth of frost penetration (Fig. 10). Minnesota with over 60 in. has the highest penetration while Texas has a range from 0 in

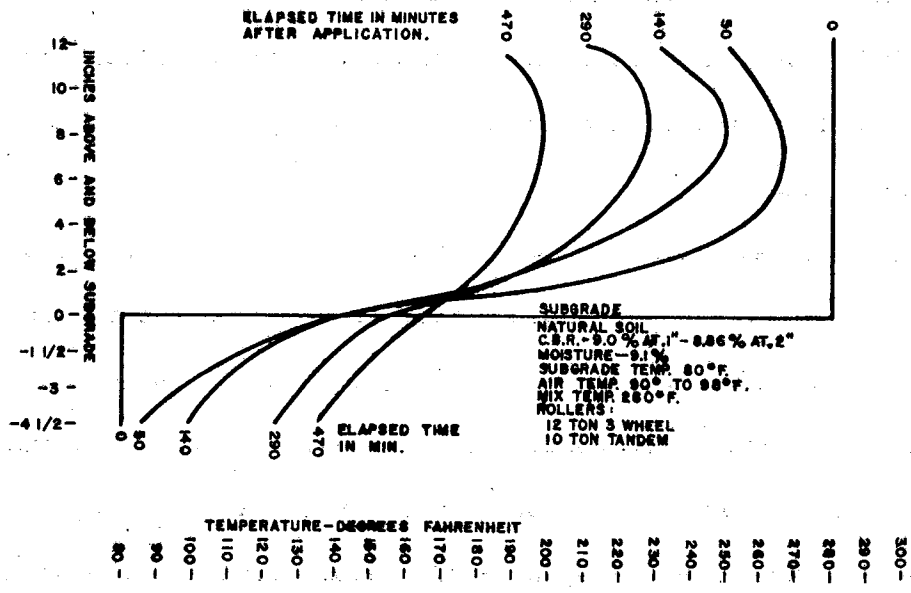


Fig. 6. Temperatures During Application of Hot Plant Mix Stabilized Base. Single Lift 12 In. Compacted Thickness (15).

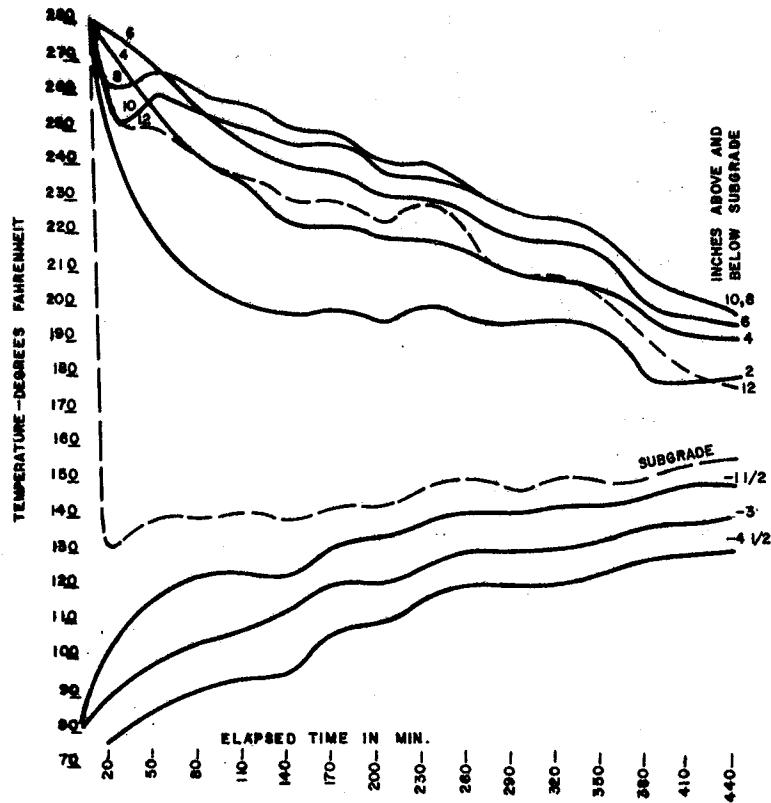


Fig. 7. Cooling Temperature During Application of Hot Plant Mix Stabilized Base. Single Lift 12 In. Compacted Thickness (15).

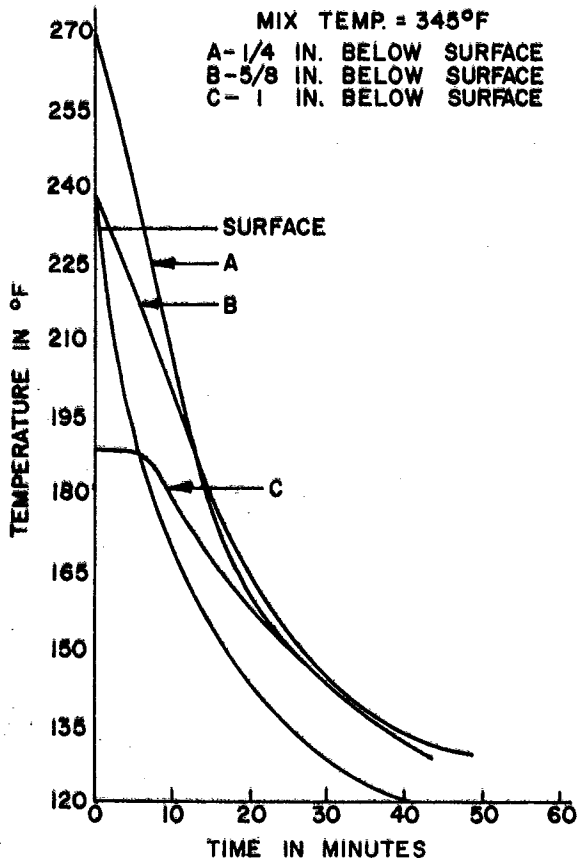


Fig. 8. Cooling Curves--Set 2, Station IV-1 (16).

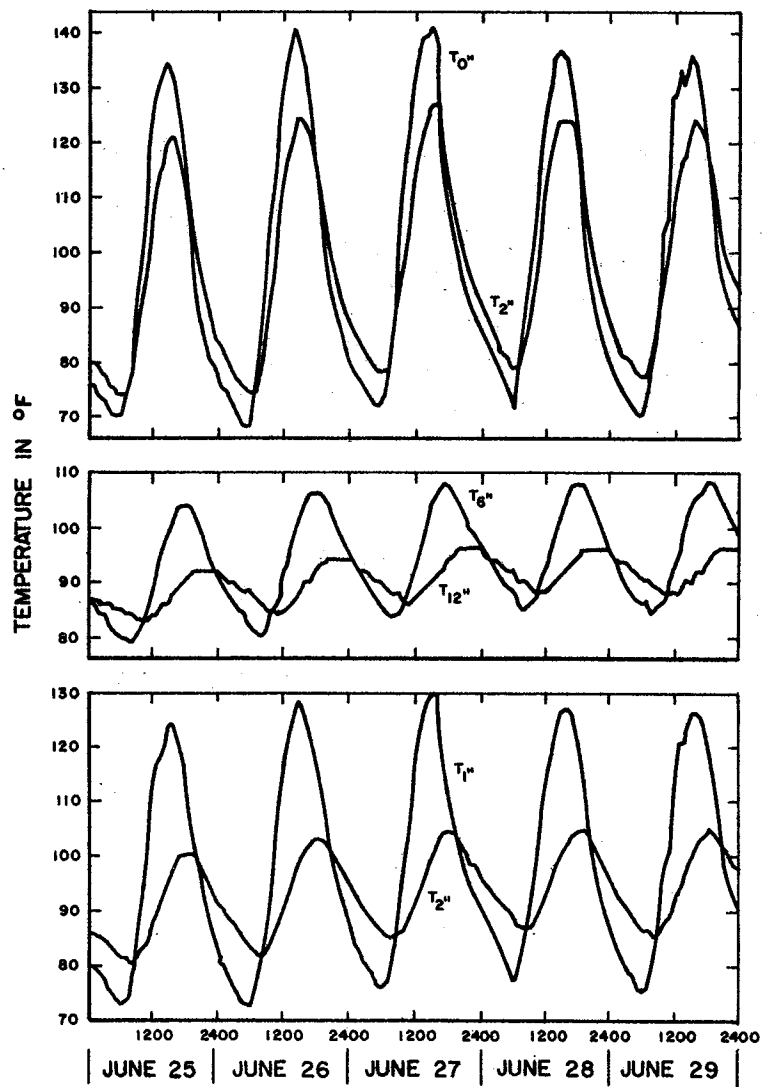


Fig. 9. Hourly Temperatures in June (17).

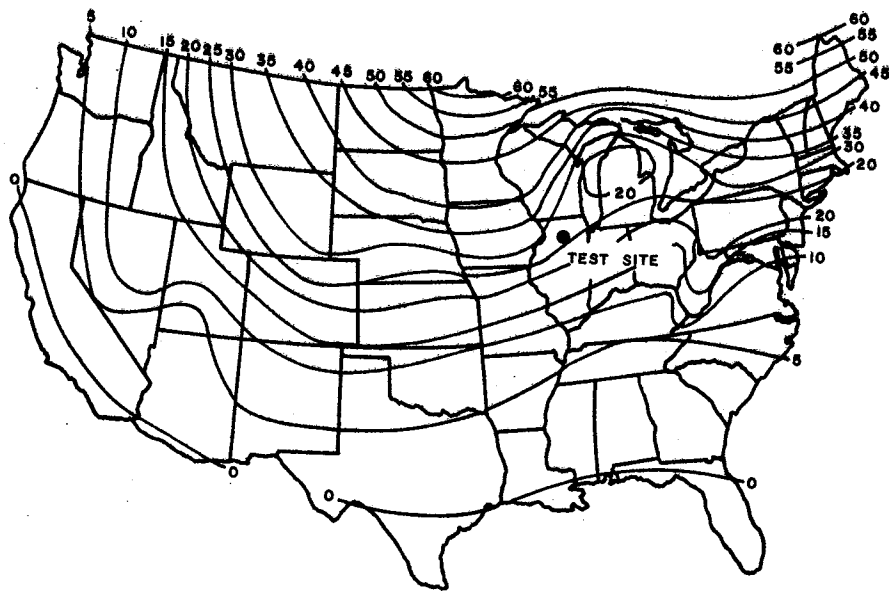


Fig. 10. Average Annual Frost Penetration, in Inches (18).

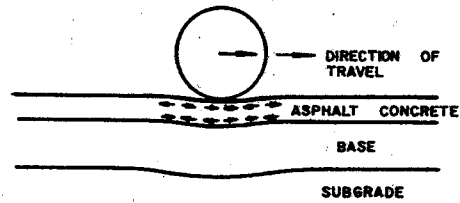
the Rio Grande Valley to a maximum of about 12 in. in the Panhandle.

It often appears that an asphaltic concrete pavement behaves erratically, i.e. cracks in one location and doesn't in another. One of the many contributing reasons for this disparity could be differences in rate of rainfall. A sudden rainfall on a very hot day could produce considerable transient thermal stress in the pavement, i.e. a thermal shock loading.

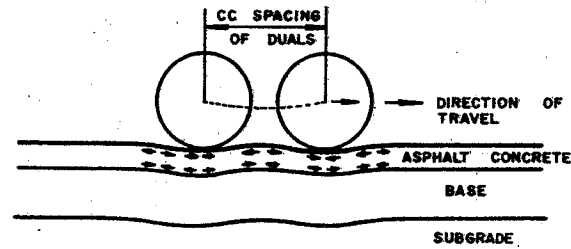
2.5 Mechanically Induced Distress

A schematic of wheel load response is shown in Fig. 11. Monismith, Secor, and Blackmer (19) have given the strain-time functionals for a 15-kip load at 4 and 20 mph (Figs. 12 and 13). The ratio of maximum compressive to maximum tensile strain in the pavement surface was about 4 for both speeds, with a cycle period of about 1.8 sec. for 4 mph and 0.4 sec. for 20 mph.

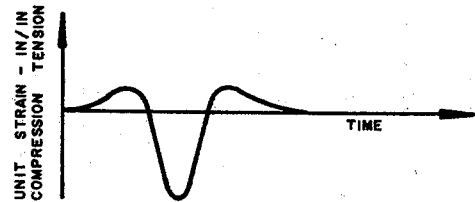
Papazian and Baker (20) stated that for the same loading and subgrade, the pavement stresses in flexible surfaces are greater than in equal thickness of more rigid asphaltic concrete pavements (Fig. 14a,b). This is probably true in most situations but observe the deflection patterns in Fig. 14c,d. If the pavement is relatively soft and the foundation is relatively rigid, the pavement is essentially in pure compression rather than flexure, hence small deflections and small stresses occur (Fig. 14c) which is contrary to the preceding generality. Another exception might be the



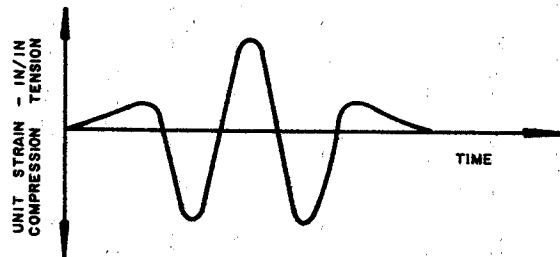
STRESSES IN ASPHALT CONCRETE
IN VICINITY OF SINGLE
AXLE LOAD



STRESSES IN ASPHALT
CONCRETE IN VICINITY OF
TANDEM AXLE LOAD



VARIATION OF STRAIN WITH
TIME AT A POINT IN SURFACE
OF ASPHALT CONCRETE DUE
TO MOVING SINGLE AXLE LOAD



VARIATION OF STRAIN WITH
TIME AT A POINT IN SURFACE
OF ASPHALT CONCRETE DUE
TO MOVING TANDEM AXLE LOAD

Fig. 11. Schematic of Strain Distribution

Single and Dual Wheel Loading.

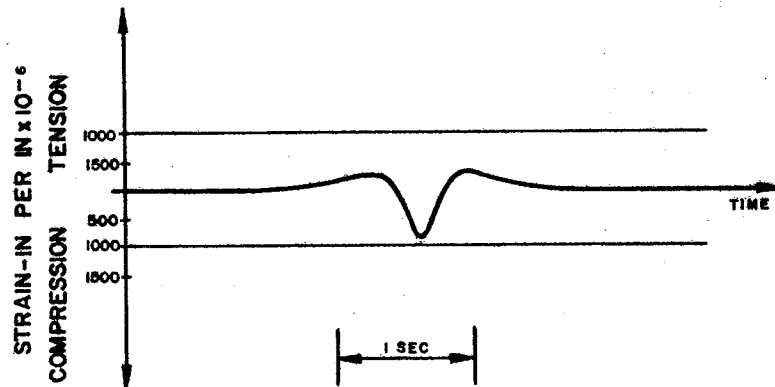


Fig. 12. Strain Variation on Surface of Pavement
 for Single Axle Truck--Creep Speed--
 (Approximately 4 mph) (19).

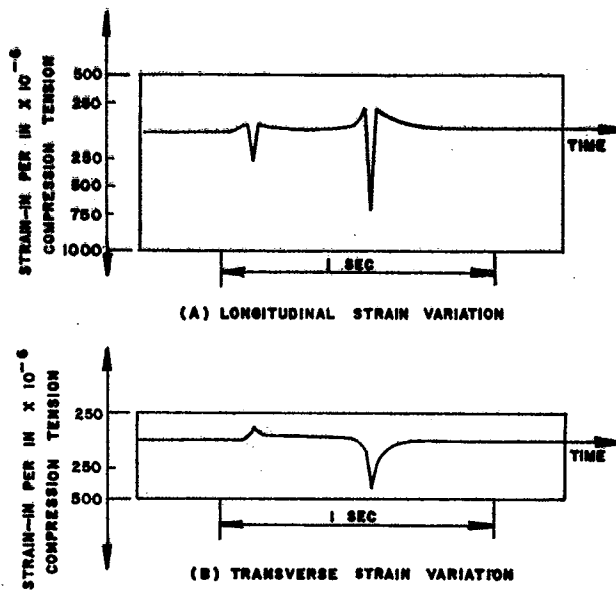
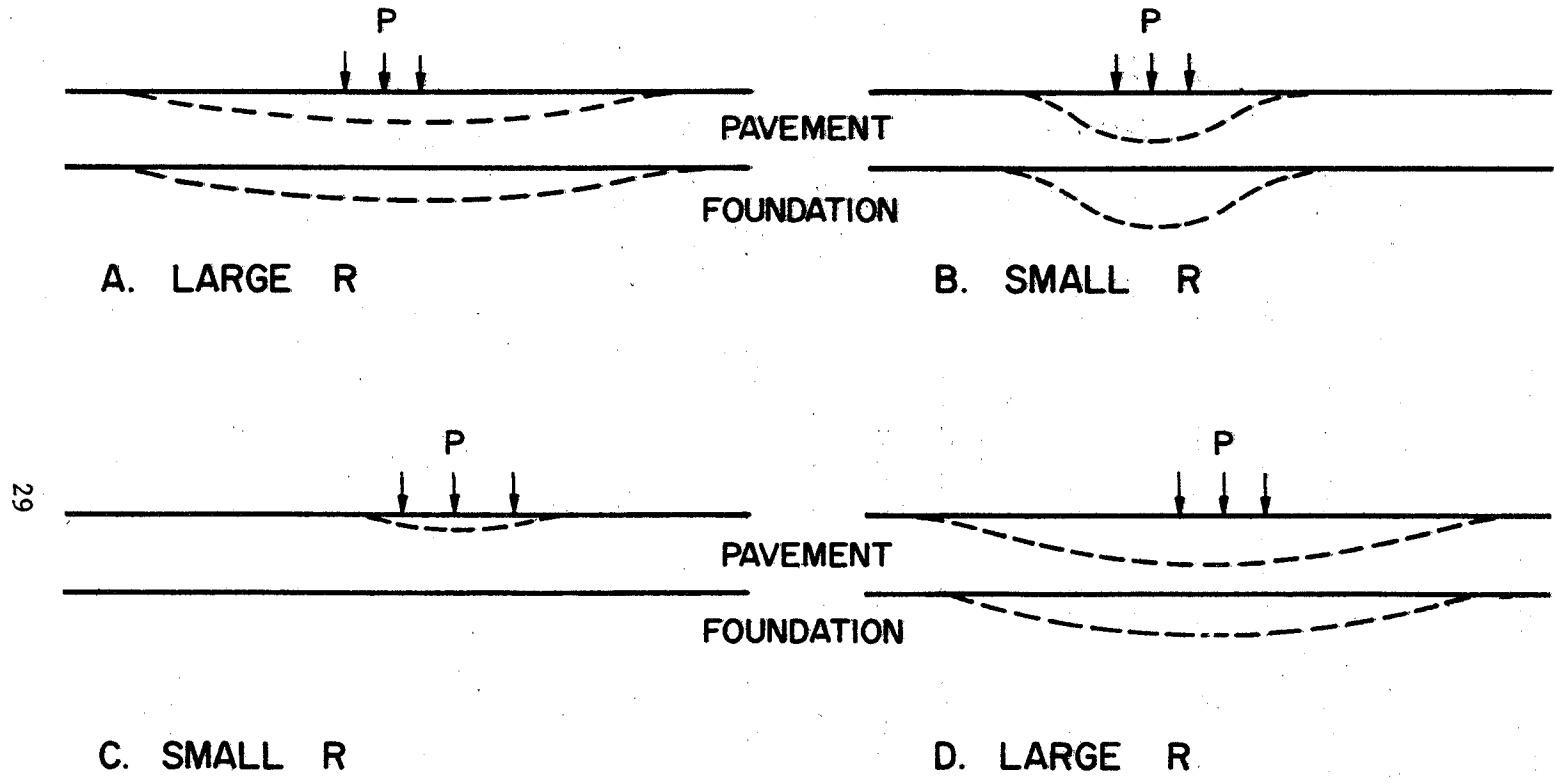


Fig. 13. Strain Variation on Surface of Pavement
for Single Axle Truck--20 mph Velocity
(19).



29

Fig. 14. Influence of Stiffness Ratio, R (ratio of pavement to foundation modulus).

placement of a stiff pavement on a very soft foundation, i.e.

Fig. 14d.

In a connected system such as a flexible pavement with base and foundation, large surface deflections do not necessarily indicate high strains in the pavement because of the resilience of the underlying structure. Actually, the induced pavement strain is a function of the radius of curvature which is a function of the second differential of the deflected surface.

Using a model analogy (Fig. 15a), Ekse (21) has determined the pressure distribution at the pavement-foundation interface for various thicknesses of asphaltic concrete (Fig. 15b). The interface pressure decreases and the radius of curvature increases considerably with increasing pavement thickness.

From Benkelman Beam data obtained on the WASHO Road Test (13), typical deflection profiles were obtained for 18-kip single axle loads (Fig. 16) and 40 kip tandem axle loads (Fig. 17). In these tests the deflection basin extended about 38 in. ahead and about 63 in. behind the wheel on a single axle. The basin extended about 42 in. ahead and about 113 in. behind the tandem wheels. It should be noted here, however, that Dunlap and Stark (22) found that the deflection basin, with a 9-kip wheel load, was over 16 feet wide in 50% of the cases they studied.

Yoder's work (23) gives some insight concerning the effect of asphaltic concrete temperature on wheel load deflections. With a

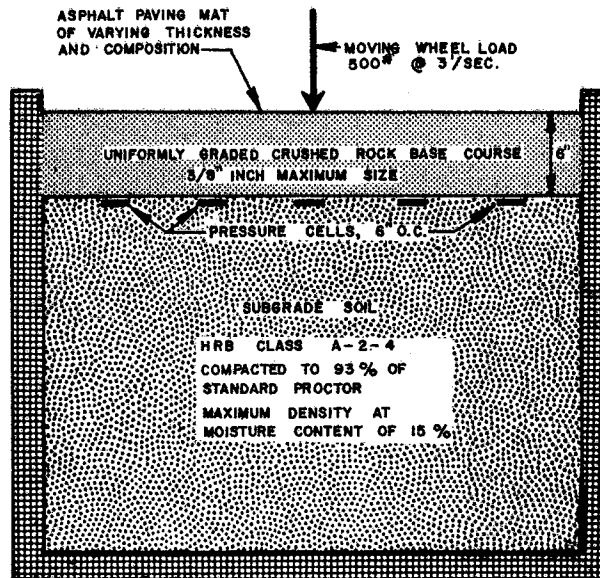


Fig. 15a. Cross Section of Laboratory Highway Test Track Showing General Scheme of Installation (21).

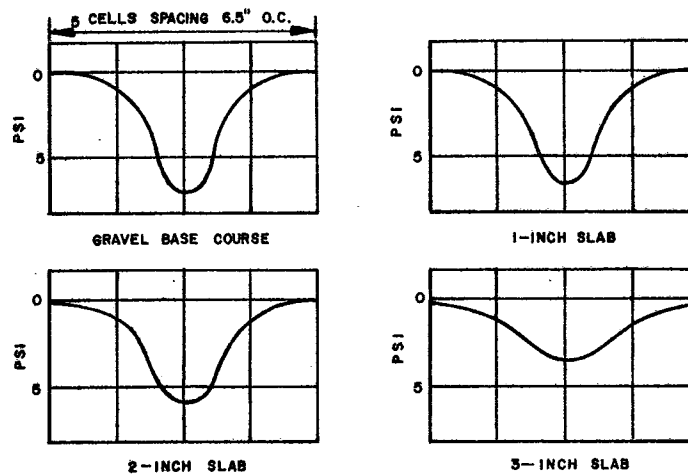


Fig. 15b. Pressure Distribution Under 500-Pound Load as Affected by Slab Thickness, Temperature at 70°F (21).

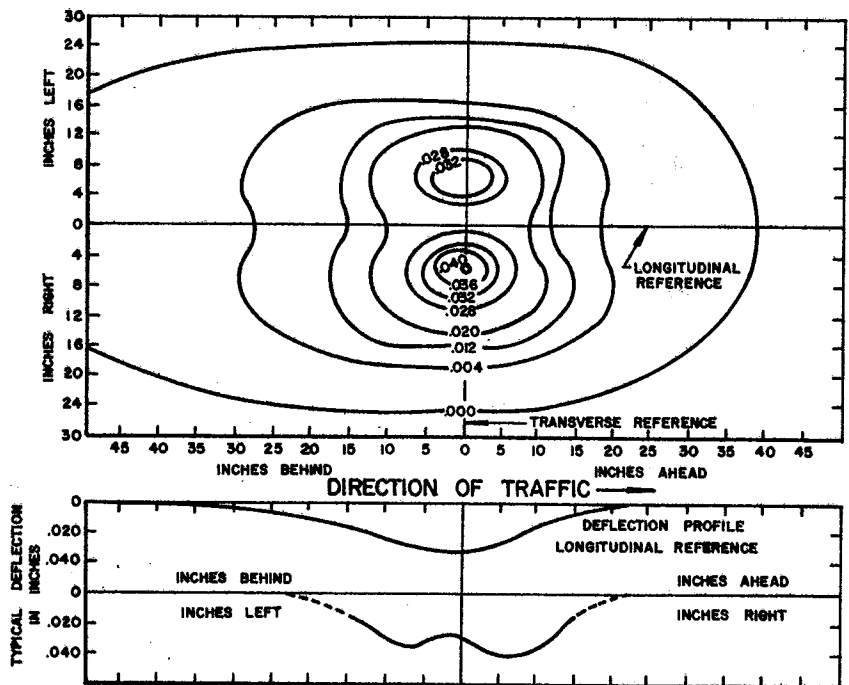
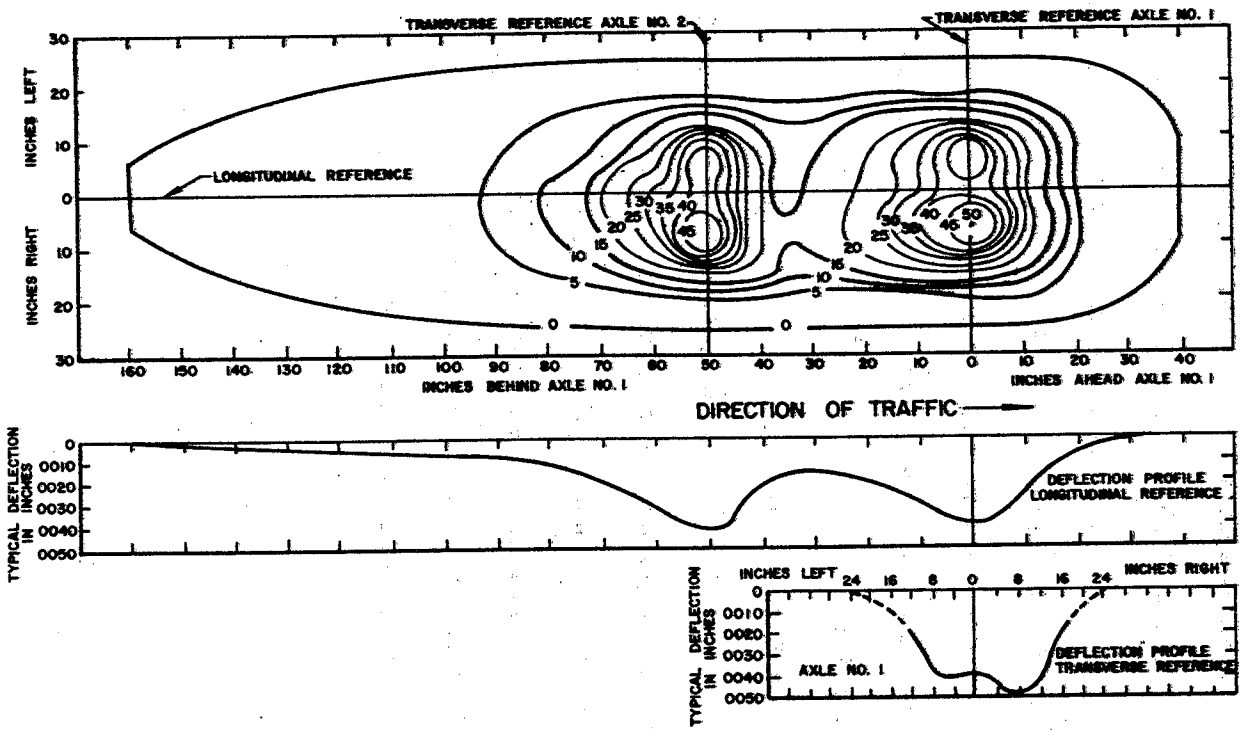


Fig. 16. Deflection Contours and Profiles 18-Kip
Single Axle Load--WASHO Road Test (13).



33

Fig. 17. Deflection Contours and Profiles 40-Kip

Tandem Axle Load-WASHO Road Test (13).

18-kip single axle load on a 4-in. lift, the average normalized deflection of the dual wheels varied almost linearly from 0.0025 in./kip at 50°F to about 0.0013 in./kip at 10°F (Fig. 18).

Yoder also found that 20% of the surface deflection could be felt at a depth of about 6 feet (Fig. 19). Hveem (24) reported foundation disturbances down to 18 feet due to pavement loads, but indicated that only the top 9 feet should be quite adequate for deflection correlations.

Finn (25) presented a survey of nine different methods that have been commonly used for determining pavement deflections in field tests. The expected accuracy of the instrumentation is not better than 0.001 in. for most of the reported methods.

Itakura and Sugawara (26) have found that the impact energy of tire chains reach 7 to 15 ft-lb when vehicles run at speeds of 25 mph and thereby cause considerable immediate damage to highways.

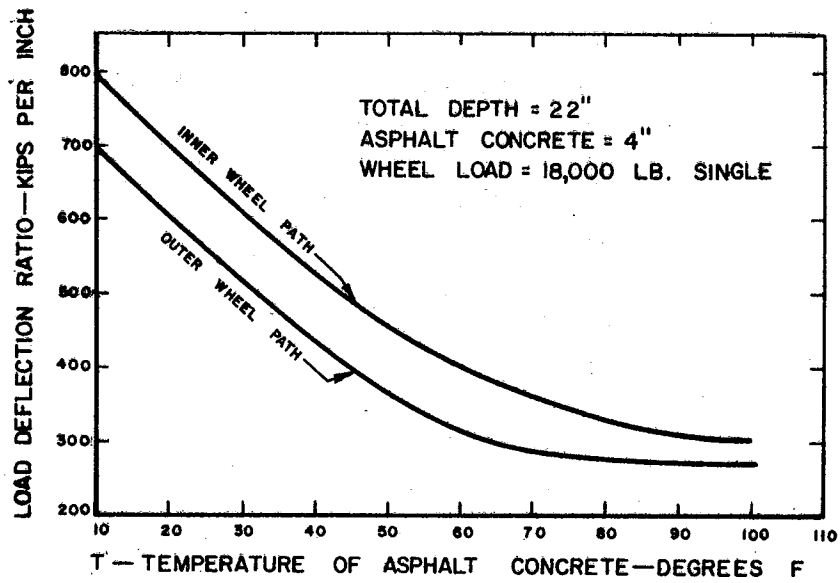


Fig. 18. Effect of Temperature on Deflection (23).

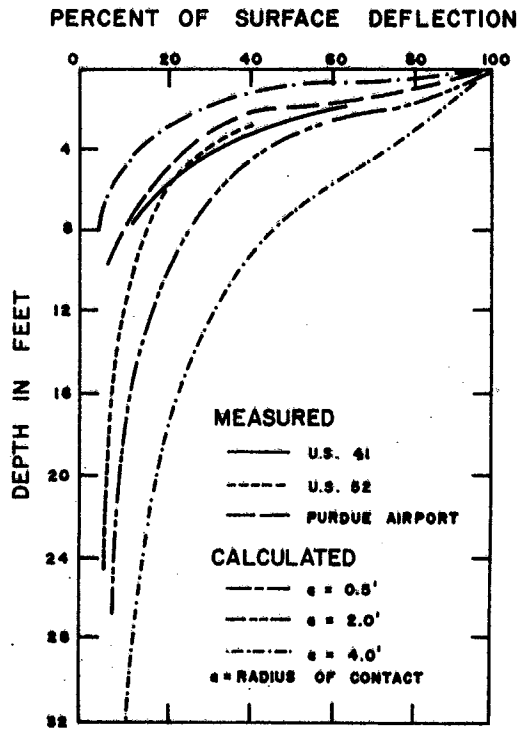


Fig. 19. Deflection Patterns (23).

CHAPTER III

THE ENERGY METHOD OF APPLIED MECHANICS

From the theory of elasticity, assuming that the material is homogeneous and isotropic, the equations for normal strain, ϵ , in terms of the displacements, u , v , and w , are:

$$\epsilon_x = \frac{\partial u}{\partial x}, \quad \epsilon_y = \frac{\partial v}{\partial y}, \quad \epsilon_z = \frac{\partial w}{\partial z} \quad (3.1a, b, c)$$

if the displacements are small. The equations for shear strain, γ , in terms of displacement are:

$$\gamma_{xy} = \frac{\partial u}{\partial y} + \frac{\partial v}{\partial x}, \quad \gamma_{xz} = \frac{\partial u}{\partial z} + \frac{\partial w}{\partial x}, \quad \gamma_{yz} = \frac{\partial v}{\partial z} + \frac{\partial w}{\partial y} \quad (3.1d, e, f)$$

In a cartesian co-ordinate system, the normal strain functionals are:

$$\epsilon_x = \frac{\sigma_x}{E} - \mu \frac{\sigma_y}{E} - \mu \frac{\sigma_z}{E} \quad (3.2a)$$

and similarly for ϵ_y, ϵ_z , where E is Young's modulus. The shear strain functionals are

$$\gamma_{xy} = \frac{\tau_{xy}}{G}, \quad \gamma_{yz} = \frac{\tau_{yz}}{G}, \quad \gamma_{xz} = \frac{\tau_{xz}}{G} \quad (3.2b, c, d)$$

Solving eq. 3.2a for the stresses:

$$\sigma_x = \frac{\mu E e}{(1+\mu)(1-2\mu)} + \frac{E \epsilon_x}{1+\mu} \quad (3.3a)$$

and similarly for σ_y, σ_z

$$\text{where } e = \epsilon_x + \epsilon_y + \epsilon_z \quad (3.3b)$$

The strain energy density, ρ , is

$$\rho = \sum_{x,y,z} \left[\frac{1}{2} \sigma_x \epsilon_x + \frac{1}{2} \tau_{xy} \gamma_{xy} \right] \quad (3.4a)$$

Consider the relation for shear modulus,

$$G = \frac{E}{2(1+\mu)} \quad (3.4b)$$

Substituting eqs. 3.3 and 3.4b into eq. 3.4a gives the relation

$$\rho = \frac{E}{2(1+\mu)} \left[\frac{\mu}{1-2\mu} e^2 + \epsilon_x^2 + \epsilon_y^2 + \epsilon_z^2 + \frac{1}{2} (\gamma_{xy}^2 + \gamma_{yz}^2 + \gamma_{zx}^2) \right] \quad (3.4c)$$

Using eqs. 3.1 and 3.3b in eq. 3.4c, the strain energy density in terms of the displacements is

$$\rho = \frac{E}{2(1+\mu)} \left[\frac{\mu}{1-2\mu} \left(\frac{\partial u}{\partial x} + \frac{\partial v}{\partial y} + \frac{\partial w}{\partial z} \right)^2 + \left(\frac{\partial u}{\partial x} \right)^2 + \left(\frac{\partial v}{\partial y} \right)^2 + \left(\frac{\partial w}{\partial z} \right)^2 + \frac{1}{2} \left(\frac{\partial u}{\partial y} + \frac{\partial v}{\partial x} \right)^2 + \frac{1}{2} \left(\frac{\partial u}{\partial z} + \frac{\partial w}{\partial x} \right)^2 + \frac{1}{2} \left(\frac{\partial v}{\partial z} + \frac{\partial w}{\partial y} \right)^2 \right] \quad (3.5)$$

In the case of plane strain,

$$\frac{\partial w}{\partial z} = \frac{\partial u}{\partial z} + \frac{\partial w}{\partial x} = \frac{\partial v}{\partial z} + \frac{\partial w}{\partial y} = 0 \quad (3.6a)$$

and in the case of plane stress,

$$\sigma_z = \tau_{yz} = \tau_{zx} = 0 \quad (3.6b)$$

The strain energy density for plane stress is

$$p_0 = \frac{E}{2(1+\mu)} \left\{ \frac{1}{1-\mu} \left[\left(\frac{\partial u}{\partial x} \right)^2 + \left(\frac{\partial v}{\partial y} \right)^2 + 2\mu \frac{\partial u}{\partial x} \frac{\partial v}{\partial y} \right] + \frac{1}{2} \left(\frac{\partial u}{\partial y} + \frac{\partial v}{\partial x} \right)^2 \right\} \quad (3.6c)$$

If the boundary forces exist, the potential, \mathbb{P} , is

$$\mathbb{P} = \int p_0 dV - \sum \int p dA \bar{u} \quad (3.7)$$

where p is the pressure, A is the area on which p acts, and \bar{u} is a generalized co-ordinate.

If a change of temperature occurs without thermal restraint,

$$\mathbb{P} = \int p_0 dV - \sum \int p u dA + \int \gamma dV \quad (3.8)$$

where γ = strain energy density due to thermal contraction.

If thermal restraints act on the system

$$P = \int \xi \, dV - \sum \int p u \, dA + \int \gamma \, dV - \int \beta \, dV \quad (3.9)$$

where β is thermal constraint energy density. The procedure to obtain a solution then is as follows. The displacements are assumed in terms of the generalized co-ordinates, using continuous functions (polynomials, Fourier series, etc.). The continuous functions are then operated on per eq. 3.1 and the results substituted in eq. 3.5. Next, eq. 3.5 is operated on by variational calculus for as many times as there are unknown constants in the continuous functions and each differential equation is set to zero to effect the minimum potential, i.e.

$$\frac{\partial P}{\partial c_i} = \frac{\partial}{\partial c_i} \int F(c_i) = 0 \quad (3.10)$$

The solution of the simultaneous equations gives the best answer in terms of given constraints, i.e. the exact solution is obtained when an infinite number of terms are used. However, judicious choice of functional form can give say 95% of the correct answer with only a few terms. This procedure can be used in linear thermoviscoelasticity by the use of a time-temperature varying modulus, but it then becomes necessary to repeat the procedure sufficient times to approximate the delayed effects by step functions if the time of loading is not brief.

CHAPTER IV

AN APPROXIMATE ENERGY SOLUTION FOR THERMAL DISTRESS

For design purposes it will be convenient to have an approximate solution for calculating the amount of thermal strain due to uniform temperature changes. One of the possible states of thermal strain is depicted schematically in Fig. 20. The energy method for obtaining a first approximation is explained as follows:

Assume that the structural integrity of the bond between the asphaltic concrete and the foundation is maintained during and after a uniform reduction in the temperature at every point in the pavement and its foundation, and assume that the modulus of the foundation, E_f , is very large with respect to the modulus of the pavement, $E_p(t, T)$ i.e.

$$\frac{E_p(t, T)}{E_f} \doteq 0 \quad (4.1)$$

The situation after the temperature reduction is illustrated in Fig. 20c.

The right hand generalized co-ordinate system given in Fig. 20a will be used. The pavement is symmetrical about the plane $x=0$.

Half the width of the highway is W and the pavement thickness is H .

The thermal problem can be transformed into an equivalent mechanical problem to simplify the analysis. This is done by first letting the foundation and the pavement freely contract, Fig. 20b, as if there were no interface bond. Then pull the pavement at $z=H$ over to the edge of the roadbed until compatibility of displacements between the foundation and the pavement exists over $z=H, x=0$ to W , as indicated in Fig. 20c.

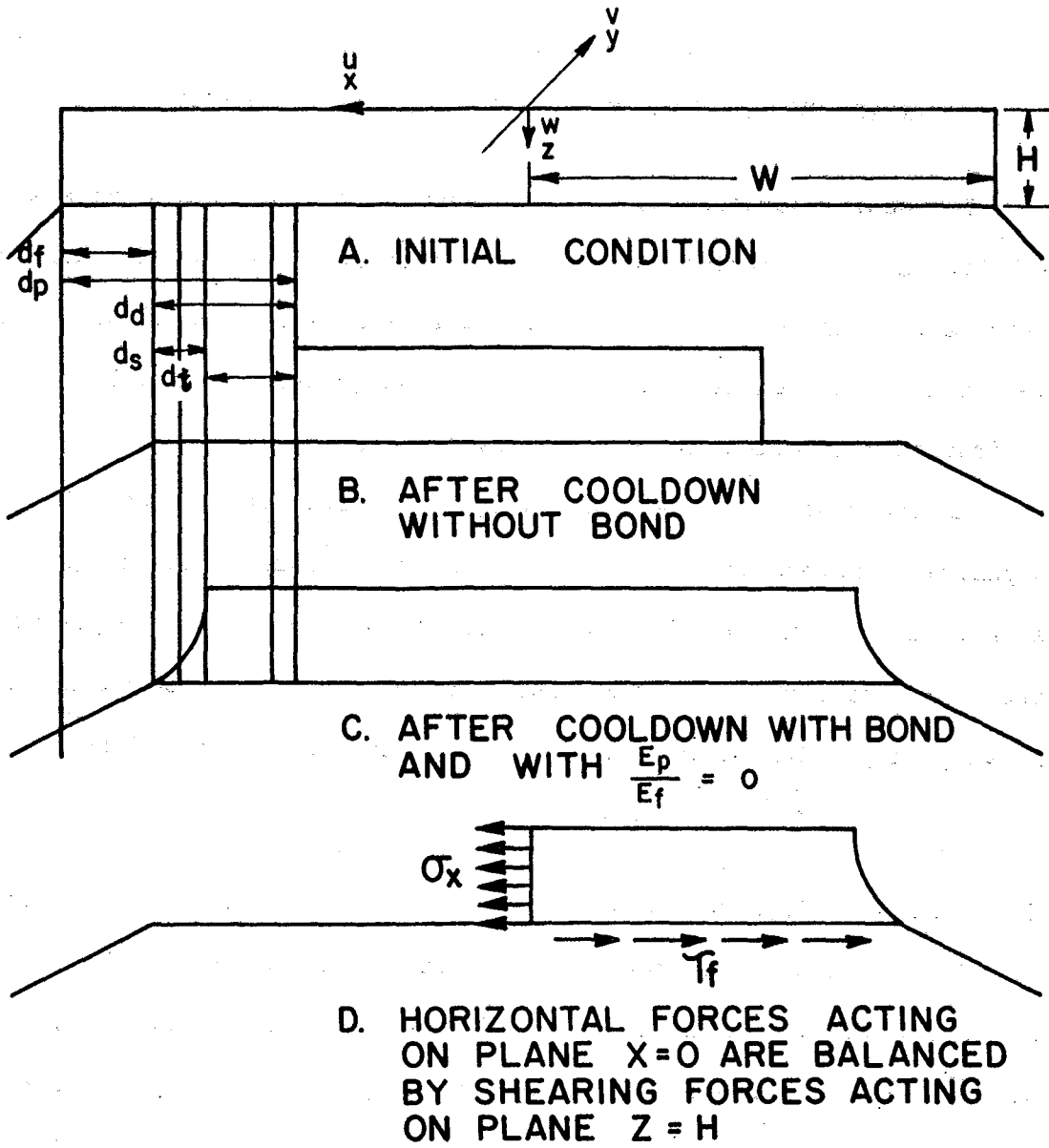


Fig. 20. Schematic on States of Thermal Distress.

From the nomenclature in Fig. 20, note that the horizontal thermal displacement of the foundation, d_f , for the case of no bond, is

$$d_f = \alpha_f W \Delta T \quad (4.2a)$$

where α is the linear coefficient of thermal expansion and ΔT is the change in temperature. ΔT is positive for a reduction in temperature. The horizontal thermal deflection of the pavement, d_p , for the case of no bond, is

$$d_p = \alpha_p W \Delta T \quad (4.2b)$$

Thus, the differential expansion, d_d , for the case of no bond, is

$$d_d = (\alpha_p - \alpha_f) W \Delta T = d_s + d_t \quad (4.3a, b)$$

and by definition, $d_s = d_d - d_t$ (4.3c)

where d_s is the deformation of shear lag and d_t is the deformation at the top surface of the pavement.

Assuming a parabolic distribution of pavement deformation, u , in the z direction at $x = W$,

$$d(W, z) = d_t + a_1 z^2 \quad (4.4a)$$

and since

$$d(w, H) = d_s, \quad a_1 = \frac{d_s - d_t}{H^2} \quad (4.4b, c)$$

and eq. 4.4a becomes

$$d(w, z) = d_s + \frac{d_s - d_t}{H^2} z^2 \quad (4.4d)$$

Using eq. 4.3c in eq. 4.4d gives

$$d(w, z) = (\alpha_p - \alpha_f) WAT - d_s + \frac{d_s}{H^2} z^2 \quad (4.5a)$$

Since the pavement is symmetrical about $x=0$, assume a parabolic distribution of deformation along x , with zero deformation at $x=0$, to wit:

$$u(x) = a_2 x^2 \quad (4.5b)$$

and since

$$u(w, z) = d(w, z) \quad (4.5c)$$

then

$$a_2 = \frac{(\alpha_p - \alpha_f) WAT - d_s + \frac{d_s}{H^2} z^2}{W^2} \quad (4.5d)$$

and therefore

$$u(x, z) = \left\{ \frac{(\alpha_p - \alpha_s) \Delta T}{W} + \alpha_s \left[\left(\frac{z}{WH} \right)^2 - \frac{1}{W^2} \right] \right\} x^2 \quad (4.6)$$

The pavement being in plane strain in the xz plane gives the boundary conditions:

$$0 = \frac{\partial v}{\partial y} = \frac{\partial v}{\partial z} + \frac{\partial w}{\partial y} = \frac{\partial v}{\partial x} + \frac{\partial u}{\partial y} \quad (4.7a)$$

Note that under these conditions, $\sigma_y \neq 0$. Since the aspect ratio of the pavement is so small, neglect the influence of the w contractions in the approximate analysis, i.e.

$$\frac{H}{W} \doteq 0 \Rightarrow 0 = \frac{\partial w}{\partial z} = \frac{\partial w}{\partial x} \quad (4.7b, c)$$

Using the boundary conditions of eqs. 4.7a, c, the strain energy density from eq. 3.5 reduces to:

$$\rho_{st} = \frac{E}{2(1+\mu)} \left[\frac{1-\mu}{1-2\mu} \left(\frac{\partial u}{\partial x} \right)^2 + \frac{1}{2} \left(\frac{\partial u}{\partial z} \right)^2 \right] \quad (4.8a)$$

Performing the indicated operations on eq. 4.6 and substituting in eq. 4.8a gives

$$\begin{aligned} \mathcal{F} = & \frac{E}{2(1+\mu)} \left\{ \frac{1-\mu}{1-2\mu} 4x^2 \left(\bar{\alpha} \frac{\Delta T}{W} + d_s \left[\left(\frac{z}{WH} \right)^2 - \frac{1}{W^2} \right] \right)^2 \right\} + \\ & \frac{E}{4(1+\mu)} \left\{ \frac{2 d_s x^2 z}{(WH)^2} \right\}^2 \end{aligned} \quad (4.8b)$$

where $\bar{\alpha} = \alpha_p - \alpha_f$ (4.8c)

The strain energy is then

$$\begin{aligned} U^e &= 2 \int_{x=0}^W \int_{z=0}^H \mathcal{F} \, dA \\ &= \frac{E}{1+\mu} \left(\frac{1-\mu}{1-2\mu} \right) \int_0^W \int_0^H \left\{ 4x^2 \left(\bar{\alpha} \frac{\Delta T}{W} + \frac{d_s z^2}{W^2 H^2} - \frac{d_s}{W^2} \right)^2 + \frac{1-2\mu}{1-\mu} \frac{2 d_s^2 x^4 z^2}{W^4 H^4} \right\} dx dz \end{aligned} \quad (4.9a)$$

Taking the first variation of eq. 4.9a with respect to d_s ,

$$\begin{aligned} \delta U^e = 0 &= \int_0^W \int_0^H \left\{ x^2 \left[2 \bar{\alpha} \frac{\Delta T}{W} \left(\frac{z^2}{W^2 H^2} - \frac{1}{W^2} \right) + 2 d_s \left(\frac{z^2}{W^2 H^2} - \frac{1}{W^2} \right)^2 \right] + \right. \\ & \left. \frac{1-2\mu}{1-\mu} \frac{d_s x^4 z^2}{W^4 H^4} \right\} dx dz \end{aligned} \quad (4.9b)$$

Performing the integration gives the result,

$$0 = -10 \bar{\alpha} \Delta T H + 8 d_s \frac{H}{W} + \frac{1-2\mu}{1-\mu} \left(\frac{3}{2} \right) \frac{W}{H} d_s \quad (4.9c)$$

Solving for d_s ,

$$d_s = \frac{20 \bar{\alpha} \Delta T H}{16 \frac{H}{W} + \frac{1-2\mu}{1-\mu} \left(\frac{3}{2}\right) \frac{W}{H}} \quad (4.9d)$$

The deformation, u , at any point can now be found by substituting eq. 4.9d in eq. 4.6:

$$u(x, z) = \left\{ \frac{\bar{\alpha} \Delta T}{W} + \left[\frac{10 \bar{\alpha} \Delta T H}{8 \frac{H}{W} + \frac{1-2\mu}{1-\mu} \left(\frac{3}{2}\right) \frac{W}{H}} \right] \left[\left(\frac{z}{WH}\right)^2 - \frac{1}{W^2} \right] \right\} x^2 \quad (4.10a)$$

Using the operator $\epsilon_x = \frac{\partial u}{\partial x}$ (4.10b)

gives the lateral strain at any point:

$$\epsilon_x(x, z) = \frac{2x \bar{\alpha} \Delta T}{W} \left\{ 1 + \left[\frac{20 H^2}{16 H^2 + \frac{1-2\mu}{1-\mu} 3 W^2} \right] \left[\frac{z^2}{H^2} - 1 \right] \right\} \quad (4.10c)$$

From eq. 4.10c the maximum thermal strain in the top surface of the pavement is

$$\epsilon_x(W, 0) = 2 \bar{\alpha} \Delta T \left\{ 1 - \frac{20 H^2}{16 H^2 + \frac{1-2\mu}{1-\mu} 3 W^2} \right\} \quad (4.11a)$$

and the maximum thermal strain at the pavement-foundation interface is

$$\epsilon_x(W, H) = 2 \bar{\alpha} \Delta T \quad (4.11b)$$

The factor of two in this last equation is a result of the parabolic assumption of the deformation in the x direction ranging from zero at the centerline to a maximum at the pavement edge. The implication here is that the deformation in the foundation varies likewise as the pavement stretches or contracts, which is a reasonable proposition.

The strain in the direction parallel to the highway centerline (see Fig. 20) is constant in the xz plane and has a value of

$$\epsilon_y = \bar{\alpha} \Delta T \quad (4.12)$$

Using eqs. 4.10c and 4.12 in the three dimensional stress-strain relation (eq. 3.3a):

$$\sigma_x(t, T, x, z) = \frac{E(t, T) \mu \bar{\alpha} \Delta T}{(1+\mu)(1-2\mu)} \left\{ \frac{2x}{W} \left[1 + \left(\frac{20H^2}{16H^2 + \frac{1-2\mu}{1-\mu} 3W^2} \right) \left(\frac{z^2}{H^2} - 1 \right) \right] \left[1 + \frac{1-2\mu}{\mu} \right] + 1 \right\}$$

where $E(t, T)$ is the time-temperature dependent viscoelastic modulus.

It can be shown that stresses calculated from eq. 4.13 are tensile if the following conditions are met:

$$\begin{aligned} \Delta T &> 0 \\ \alpha_p &> \alpha_f \\ \frac{H^2}{W^2} &< \frac{3}{4} \left(\frac{1-2\mu}{1-\mu} \right) \end{aligned}$$

In practical cases all three conditions will be satisfied.

The determined biaxial state of stress points out the need for the biaxial strip test (27) for ascertaining the biaxial tensile viscoelastic modulus and the biaxial tensile failure strength of mixtures.

Consider now the half-pavement shown in Fig. 20d. The foundation shearing resistance, τ_f , acting on the bottom surface of the pavement, is mobilized by the contraction of the pavement. Its value is zero at the center, where the horizontal displacement is zero, and is probably a maximum at the edge, where the horizontal displacement is a maximum. As a first approximation, it is assumed that τ_f is a linear function of x , that is

$$\tau_f = cx \quad (4.14)$$

where c is a constant to be determined from equilibrium conditions.

For equilibrium,

$$\int_0^H \sigma_x(t, T, 0, z) dz = \int_0^W \tau_f dx \quad (4.15)$$

By putting eqs. 4.13 (with $x=0$) and 4.14 in eq. 4.15, integrating between the limits shown, and solving the resulting equation for c , one obtains the following expression for the shear stress,

τ_f :

$$\tau_f = \frac{2E(t, T) \mu \bar{\alpha} \Delta TH}{(1+\mu)(1-2\mu)W^2} x \quad (4.16)$$

Thus, the maximum value of the shear stress acting on the bottom surface of the pavement is

$$\tau_f(\text{MAX}) = \frac{2 E (t, T) \mu \bar{\alpha} \Delta T H}{(1 + \mu)(1 - 2\mu) W} \quad (4.17)$$

The finite element method would have been used in the thermal analysis since it is convenient to use for the state of plain strain; however, with the relation between the variables unknown, a computer run would be required each time a change in any of the variables is considered. At best the determined relations might be sensed after the development of numerous parametric curves from a multitude of computer runs. On the other hand, the use of the finite element method is considerably more efficient than the energy method for those problems which are one time affairs.

CHAPTER V

THERMAL DISTRESS WITH VARIABLE TEMPERATURE

5.1 Distribution of Normal Stress and Strain in the Asphaltic Concrete Layer

Alexander (2) developed perhaps the most comprehensive data now available for the mechanical response of a commonly used asphaltic concrete. He performed creep, relaxation, and constant strain rate tests on uniaxial specimens in tension and compression at various temperatures and load levels. Using the concept of time-temperature shift factors, Alexander's data for compliance and modulus were reduced and the results are given in Fig. 21 and 22.

The equation for the modulus is

$$E(t, T) = (2.5 \times 10^4) \left(\frac{t}{a_T} \right)^{-0.370} \quad (5.1a)$$

where time, t , is in seconds, and the modulus has units of psi. Approximating the curve for the master shift factors by a straight line gives the relation

$$a_T = (9.11 \times 10^5) (0.845)^T \quad (5.1b)$$

where the shift factor, a_T , is a numeric and the temperature, T , is in °F.

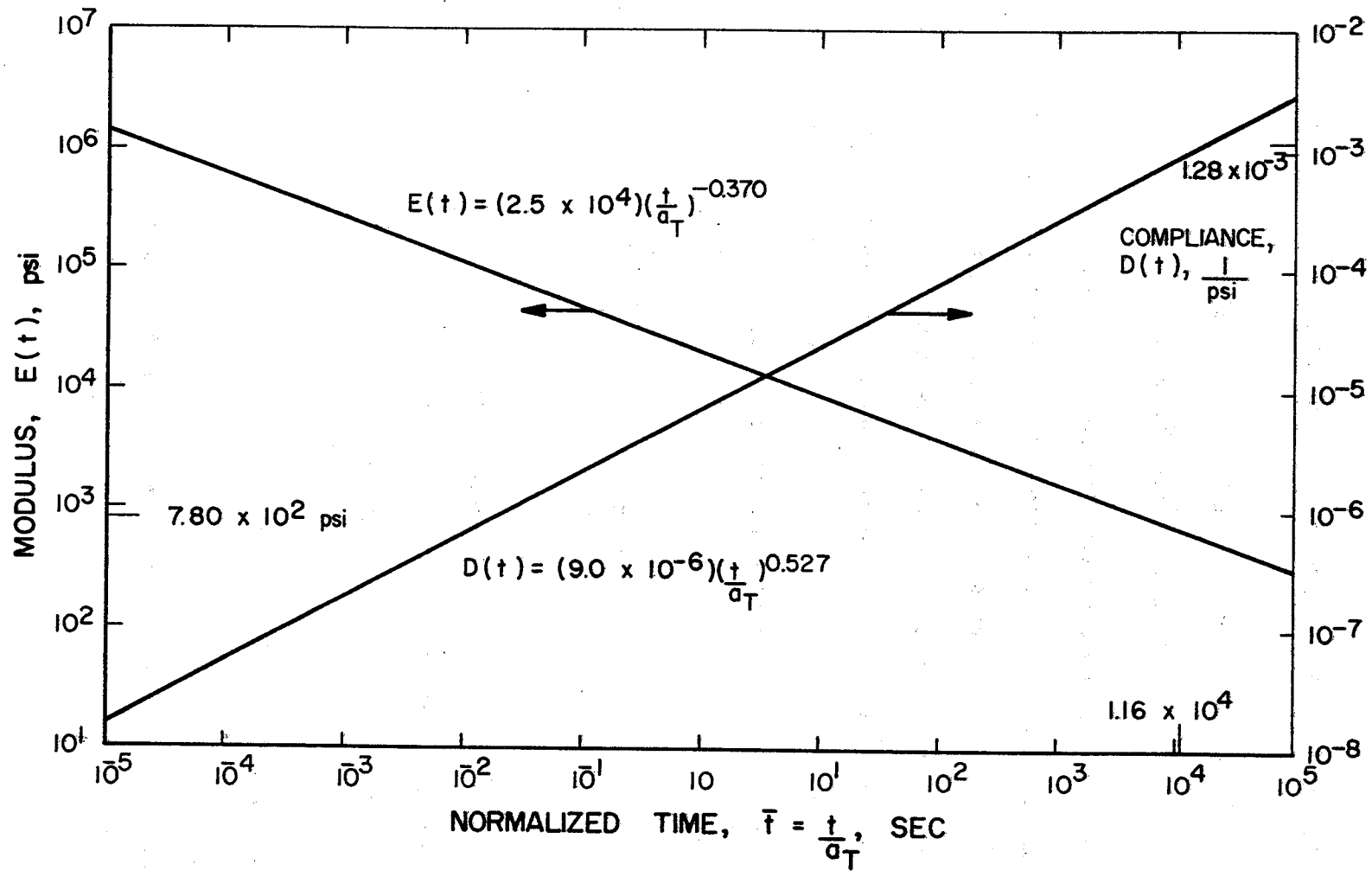


Fig. 21. Master Modulus and Compliance.

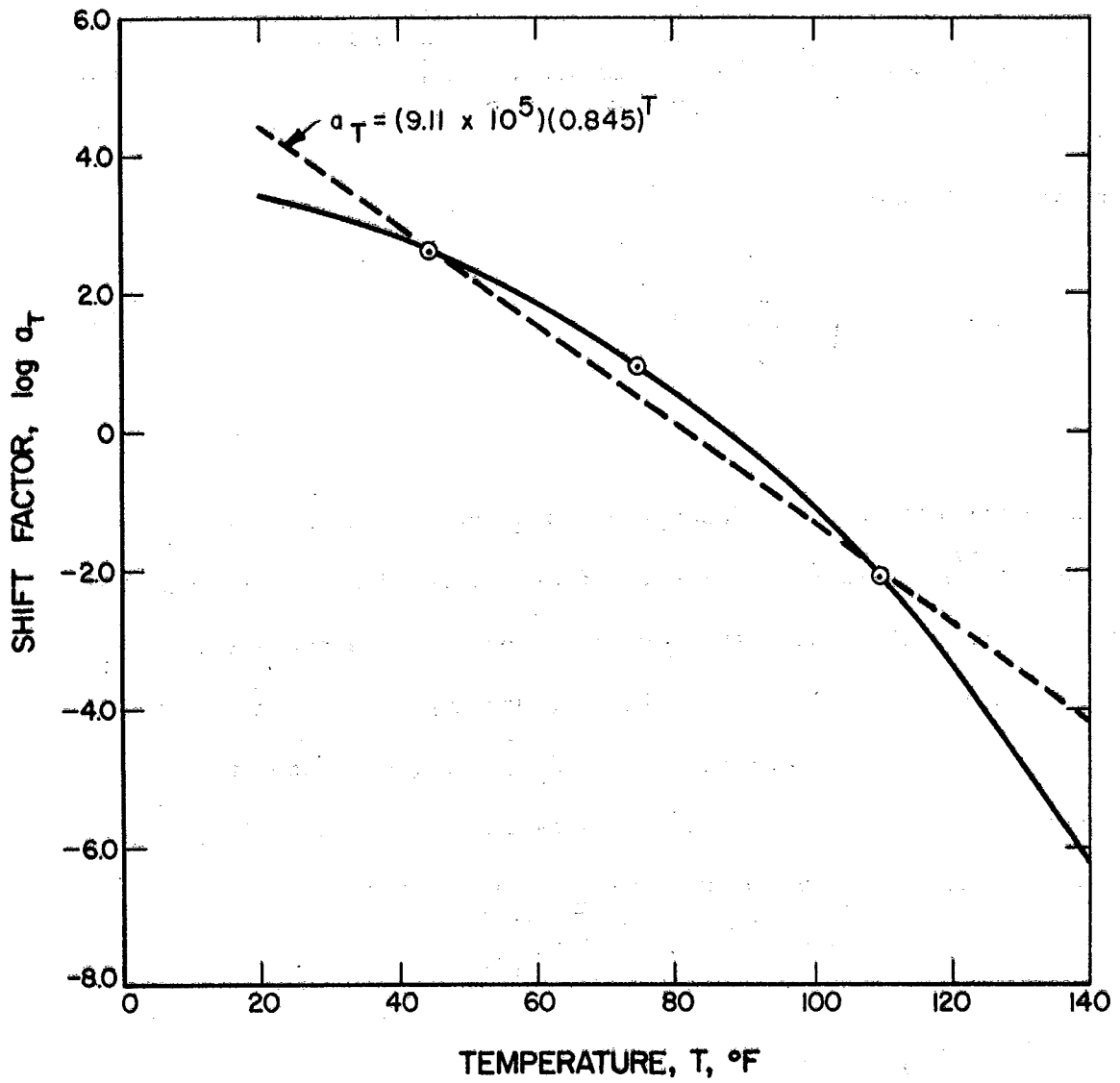


Fig. 22. Master Shift Factors.

Eqs. 5.1a, b can be combined to give

$$E(t, T) = (2.5 \times 10^4) \left[\frac{t}{(9.11 \times 10^8)(0.845 T)} \right]^{-0.370} \quad (5.1c)$$

or, in functional form:

$$E(t, T) = c_1 \left[\frac{t}{c_3 c_4 T} \right]^{c_2} \quad (5.1d)$$

Suppose a pavement and its foundation to be at a uniform initial temperature, T_L . Some time later, after a reduction in air temperature, the temperature distribution in the pavement is assumed to be curvilinear, as indicated in Fig. 23, varying from a minimum value of T_U at the top, to a maximum value of T_L at the bottom, while the temperature in the foundation remains at its initial value, T_L .

The assumed temperature distribution in the pavement is given by

$$T(y) = T_U + \bar{T} \frac{y^2}{H^2} \quad (5.2a)$$

where $\bar{T} = T_L - T_U$

The change in temperature from the initial value at any point in the pavement is $\Delta T = T_L - T(y)$

$$\text{or } \Delta T = \bar{T} \left(1 - \frac{y^2}{H^2} \right)$$

(5.2b)

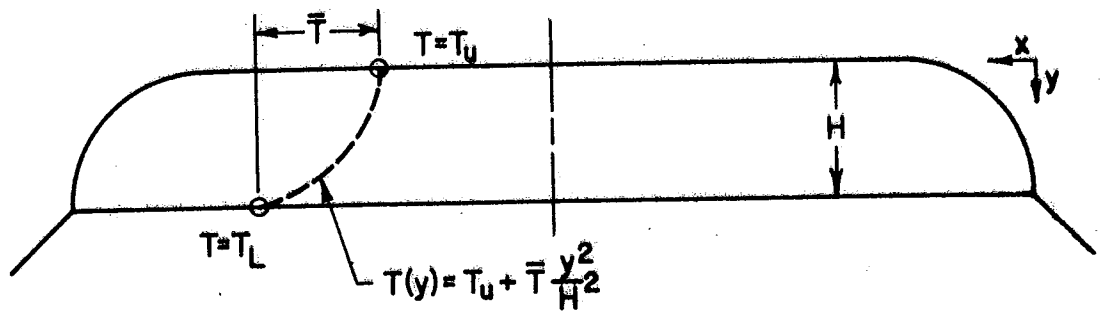


Fig. 23. Schematic of Non-uniform Temperature Distribution in the Flexible Pavement.

If the foundation is considered rigid, the thermal strain in the pavement is

$$\epsilon = \alpha_p \Delta T \quad (5.3a)$$

or using eq. 5.2d

$$\epsilon(y) = \alpha \bar{T} \left(1 - \frac{y^2}{H^2} \right) \quad (5.3b)$$

For a biaxial stress condition

$$\sigma(y, t, T) = \frac{E(t, T) \epsilon(y)}{1 - \mu} \quad (5.4a)$$

then using eq. 5.1d, the thermoviscoelastic stress is

$$\sigma(y, t, T) = c_1 \left(\frac{t}{c_3 c_4 T} \right)^{c_2} \frac{\alpha \bar{T}}{1 - \mu} \left(1 - \frac{y^2}{H^2} \right) \quad (5.4b)$$

5.2 Shear Distress at the Pavement Foundation-Interface

The sum, P , of the tensile forces acting on the plane, , in the pavement must equal the sum of the shear forces acting on the undersurface of the pavement. Then,

$$P = \int_0^H \sigma(y, t, T) dy \quad (5.5a)$$

Substituting eqs. 5.2c and 5.4b into eq. 5.5a gives

$$P = \frac{c_1 t^{c_2} \alpha \bar{T}}{c_3 c_4 c_2 (T_L - \bar{T}) (1-\mu)} \int_0^H c_4^{-c_2 \bar{T} \frac{y^2}{H^2}} \left(1 - \frac{y^2}{H^2}\right) dy \quad (5.5b)$$

The integration can be simplified by the use of a particular series expansion, which in functional form is to wit:

$$a^x = 1 + x \ln a + \frac{(x \ln a)^2}{2!} + \frac{(x \ln a)^3}{3!} + \dots \quad (5.5c)$$

$$\text{Let } B \equiv \frac{c_1 t^{c_2} \alpha \bar{T}}{c_3 c_4 c_2 (T_L - \bar{T}) (1-\mu)} \quad (5.5d)$$

$$b \equiv -c_2 \bar{T} \ln c_4 \quad (5.5e)$$

then eq. 5.5b becomes

$$P = B \int_0^H \left[1 + b \frac{y^2}{H^2} + \frac{\left(\frac{by^2}{H^2}\right)^2}{2!} + \frac{\left(\frac{by^2}{H^2}\right)^3}{3!} + \dots \right] \left[1 - \frac{y^2}{H^2} \right] dy \quad (5.6a)$$

Performing the integration and substituting the limits gives

$$P = BH \left[\frac{2}{3} + b \left(\frac{1}{3} - \frac{1}{5} \right) + \frac{b^2}{2!} \left(\frac{1}{5} - \frac{1}{7} \right) + \frac{b^3}{3!} \left(\frac{1}{7} - \frac{1}{9} \right) + \frac{b^4}{4!} \left(\frac{1}{9} - \frac{1}{11} \right) + \dots \right] \quad (5.6b)$$

which can be simplified to

$$P = \frac{2BH}{3} + 2BH \sum_{n=1}^N \frac{b^n}{n!(4n^2 + 5n + 3)} \quad (5.6c)$$

Using eqs. 5.5d and 5.5e in 5.6c gives the explicit relation:

$$P(t, T) = \frac{2Hc_1 t^{c_2} \alpha \bar{T}}{(1-\mu)c_3 c_4 c_2 (T_L - \bar{T})} \left[\frac{1}{3} + \sum_{n=1}^N \frac{(-c_2 \bar{T} \ln c_4)^n}{n!(4n^2 + 5n + 3)} \right] \quad (5.7a)$$

As in the case of a uniform reduction in temperature previously treated (Chapter IV), shear stresses, τ_f , acting on the bottom of the pavement resist its contraction. Again, it is assumed that the distribution of τ_f is linear, that is,

$$\tau_f = cx$$

where C is to be determined from the equilibrium condition,

$$P = \int_0^w \tau_f dx = \int_0^w cx dx$$

Thus,

$$c = \frac{2P}{w^2}$$

and

$$\tau_f = \frac{2P}{w^2} x \quad (5.7b)$$

It follows that the maximum value of the shear stress acting on the bottom surface of the pavement is

$$\tau_f(\text{MAX}) = \frac{2P}{w} \quad (5.7c)$$

where P is given by eq. 5.7a.

5.3 Peel Distress

From a search of the literature it did not appear that the subject of peel has received attention in regard to asphaltic concrete highway studies. A schematic of the peel mechanism is shown by the

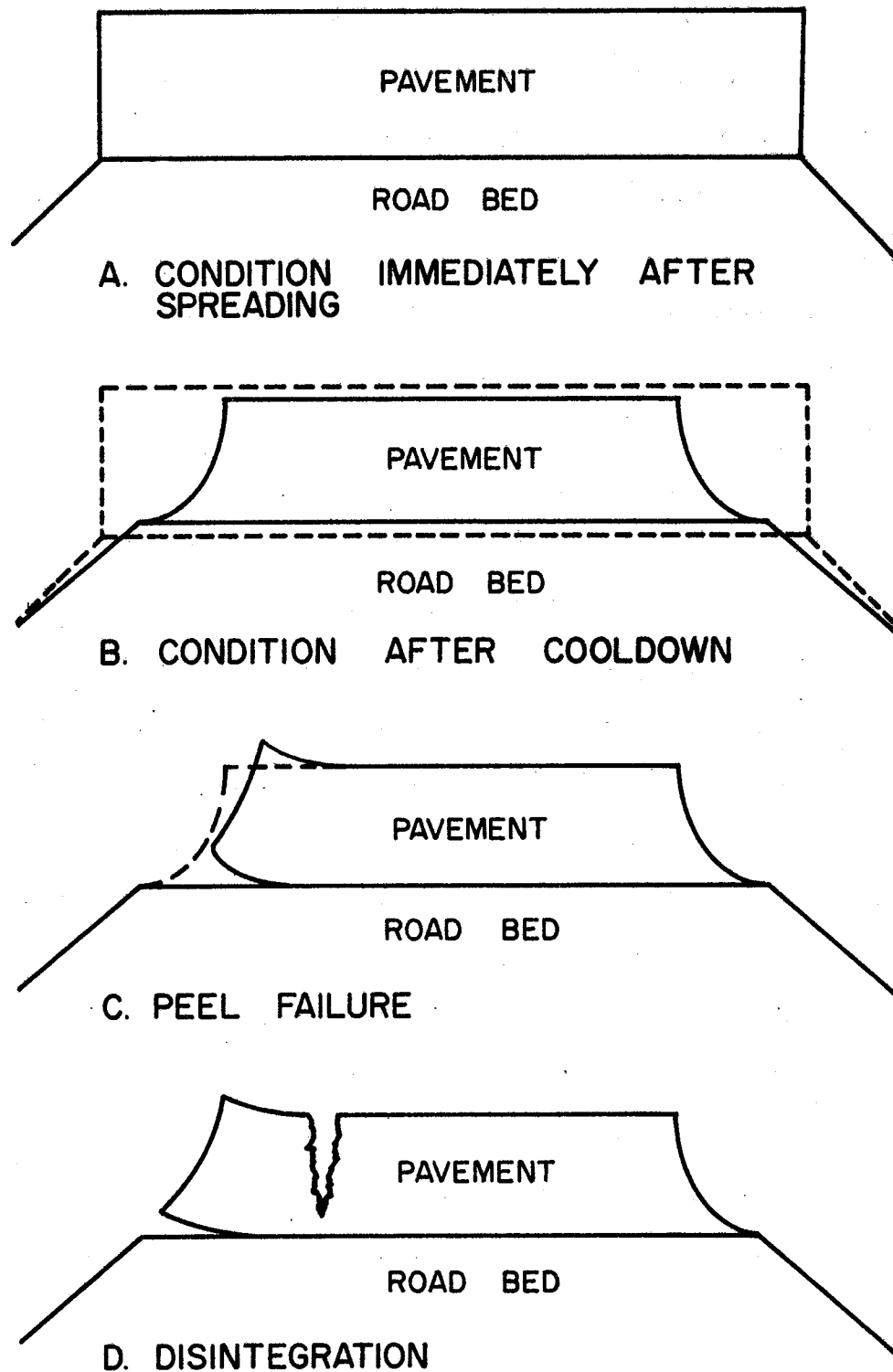


Fig. 24. Progression of Peel Mechanism.

exaggerated displacement in Fig. 24. It is of interest that the strip back test (ASTM D903-49) is commonly used in the field of solid propellant motor design for assessment of debonding between the propellant and the case. The climbing drum test (ASTM D1718-60T) modified by using a drum of very large radius might possibly serve the pavement designer. This is because the peel angle occurring during a debond failure because of thermal distress must be very small because of the tare (dead weight) of the pavement. Mylonas (28) has given an elastic analysis of the peel tests.

As a vivid illustration of peel failure, it is worth recalling the "show and tell" demonstrations popular when the epoxys first became commercially available (circa 1948). In those tests two steel blocks having a one square inch cross section were bonded together with a thin (0.005 in.) film of epoxy. One block was connected to a chain tied around an automobile. While the film would stand the direct stress of several tons, without a normal load on the film the two blocks could be pryed apart with a screwdriver causing a peel failure due to application of only a few pounds.

It seems probable that precisely the same sort of thing is happening to flexible pavements. Here, however, the damage is accentuated because after the thermal distress causes the initial peel or debond, the response of the pavement due to mechanical load becomes more severe. Once the crack has propagated through the pavement, the pavement first separates and then disintegrates quite rapidly. A rather extreme example of separation is shown in Fig. 25.

The moment, \bar{m} , caused by the nonlinear thermal strain distribution can be expressed as

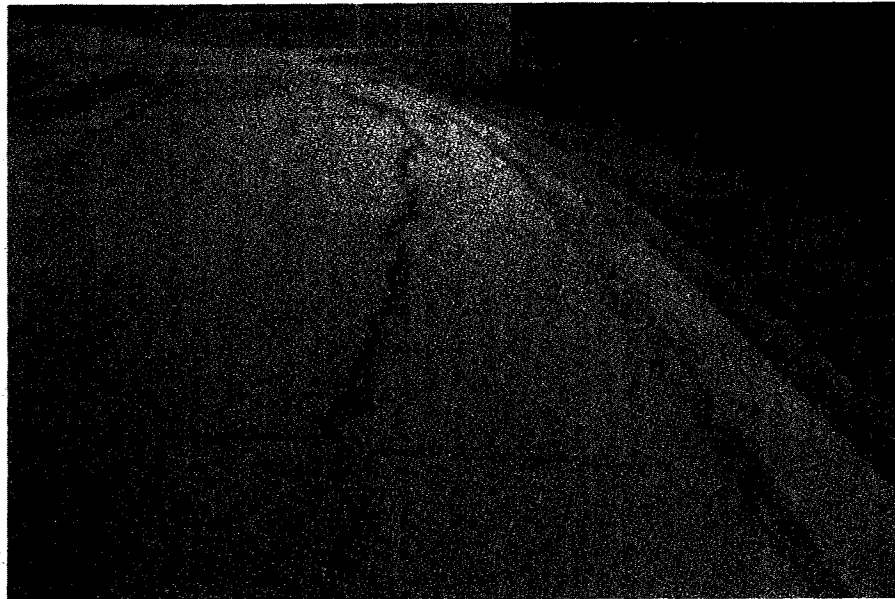


Fig. 25 Separation Due to Foundation Shift
(Frontage Road near New Braunfels)*

* Photograph courtesy of E. R. Hargett, Texas Transportation Institute.

$$\bar{m} = \int_0^H y \sigma(y, t, T) dy \quad (5.8a)$$

Carrying through with the indicated operation in the same manner as in the preceding section gives the result

$$\bar{m} = BH^2 \left[\frac{1}{4} + b \left(\frac{1}{4} - \frac{1}{6} \right) + \frac{b^2}{2!} \left(\frac{1}{6} - \frac{1}{8} \right) + \frac{b^3}{3!} \left(\frac{1}{8} - \frac{1}{10} \right) + \dots \right] \quad (5.8b)$$

which can be simplified to

$$\bar{m} = \frac{BH^2}{4} + \frac{BH^2}{2} \sum_{n=1}^N \frac{b^n}{n!(n^2+3n+2)} \quad (5.8c)$$

or in explicit form to

$$\bar{m}(t, T) = \frac{c_1 t^{c_2} \alpha \bar{T} H^2}{2c_3 c_4 c_2 (T_2 - \bar{T}) (1-\mu)} \left[\frac{1}{2} + \sum_{n=1}^N \frac{(-c_2 \bar{T} \ln c_4)^n}{n!(n^2+3n+2)} \right] \quad (5.9a)$$

Since this moment was calculated from a base line at the top surface of the pavement, the effective moment arm is at a distance of three-fourths of the pavement depth. The moment felt by the interface is therefore one-third the moment calculated, i.e.

$$m(t, T) = \frac{\bar{m}(t, T)}{3} \quad (5.9b)$$

Using the free body diagram shown in Fig. 23, the total peel moment,

M , is

$$M(t, \tau) = m(t, \tau) - \frac{\rho H}{.144} \frac{x^2}{2} \quad (5.9c)$$

CHAPTER VI

DISCUSSION OF RESULTS

6.1 General

In the discussion to follow, the following typical material properties and data will be used.

$$E_p(t, \tau) = (2.5 \times 10^4) \left(\frac{t}{a_\tau} \right)^{-0.370} \text{ psi} \quad (\text{from Fig. 21}) \quad (6.1a)$$

$$a_\tau = (9.11 \times 10^5) (0.845^\tau) \quad (\text{from Fig. 22}) \quad (6.1b)$$

$$\mu_p = 0.4 \quad (6.1c)$$

$$\alpha_s = 4 \times 10^{-6} \frac{\text{in.}}{\text{in.} \cdot ^\circ\text{F}} \quad (6.1d)$$

$$\alpha_p = 14 \times 10^{-6} \frac{\text{in.}}{\text{in.} \cdot ^\circ\text{F}} \quad (6.1e)$$

$$W = 6 \text{ ft.} \quad (6.1f)$$

$$\rho = 150 \text{ pcf} \quad (6.1g)$$

The coefficient of thermal expansion for the asphaltic concrete is taken from the data given by Monismith, Secor and Secor (5). They found that for a particular asphaltic concrete having a density of 152 pcf, the coefficient was linear over the range of -10 to 70°F.

More precisely, they gave the equation

$$\alpha_p = (11.8 + 0.04T)(10^{-6}) \frac{\text{in.}}{\text{in.} \cdot ^\circ\text{F}} \quad (6.1h)$$

where T is the temperature in $^\circ\text{F}$. The width chosen is one-half of the usual width of a traffic lane.

6.2 Equilibrium Thermal Distress

For a 12 in. lift and a 50°F ambient temperature difference, the shear lag deformation computed from eq. 4.9d is

$$d_s = \frac{20(10 \times 10^{-6})(50)}{\frac{16(12)}{6(12)} + \frac{6(12)}{2}} = 0.00027 \text{ in.} \quad (6.2a)$$

and the differential displacement is

$$d_d = (10 \times 10^{-6})(6)(12)(50) = 0.036 \text{ in.} \quad (6.2b)$$

If the lift was only 2 in. thick,

$$d_s = \frac{20(10 \times 10^{-6})(50)(12)}{\frac{16(12)}{6(12)} + \frac{0.2(3)(6)(12)}{0.6(12)}} = 0.014 \text{ in.} \quad (6.2c)$$

and the differential displacement is the same.

This calculation shows that the thermal displacement of the wearing course is 61% and 99% of the displacement at the pavement-foundation interface for 12 in. and 2 in. lifts, respectively.

Therefore, the thicker the pavement lift, the less stringent will be the thermal strain requirement of the wearing course.

Using eq. 4.10c, the thermal strain at any point in a 4 in. lift with a 50°F ambient temperature change, for example, is

$$\epsilon_x(x,z) = 2 \times \frac{(10^{-5})(50)}{72} \left\{ 1 + \left(\frac{20(4^2)}{16(4^2) + 72^2} \right) \left(\frac{z^2}{4^2} - 1 \right) \right\} \quad (6.2d)$$

The maximum strain in the wearing course is

$$\epsilon_x(w,0) = 2(10^{-5})(50) \left\{ 1 - \frac{20(4^2)}{16(4^2) + (72^2)} \right\} = 941 \times 10^{-6} \frac{\text{in.}}{\text{in.}} \quad (6.2e)$$

and the maximum strain at the pavement-foundation interface is

$$\epsilon_x(w,H) = 2(10^{-5})(50) = 1000 \times 10^{-6} \frac{\text{in.}}{\text{in.}} \quad (6.2f)$$

From the preceding results and using eq. 4.13, the maximum stresses in the wearing course and at the interface are

$$\sigma_x(t,T) = \frac{E(t,T)(0.4)}{1.4(0.2)} \left\{ \epsilon_x(x,z) \left(1 + \frac{0.2}{0.4} \right) + 0.5 \epsilon_x(w,H) \right\} \quad (6.2g)$$

$$\sigma_x(t,T) = (27.3 \times 10^{-4}) E(t,T) \text{ wearing course} \quad (6.2h)$$

$$\sigma_x(t,T) = (28.6 \times 10^{-4}) E(t,T) \text{ interface} \quad (6.2i)$$

Assuming the final temperature is 20°F and one hour is required to reach thermal equilibrium,

$$a_T = (9.11 \times 10^5)(0.845^{20}) = 6.51 \times 10^5 \quad (6.2j)$$

$$E(t, \tau) = (2.5 \times 10^4) \left(\frac{3600}{6.51 \times 10^5} \right)^{-0.370} = 17.1 \times 10^4 \text{ psi} \quad (6.2k)$$

which gives

$$\sigma_x(t, \tau) = 466 \text{ psi} \quad \text{wearing course} \quad (6.2l)$$

$$\sigma_x(t, \tau) = 490 \text{ psi} \quad \text{interface} \quad (6.2m)$$

Summarily, for the given conditions the pavement will crack if the material does not have a biaxial ultimate tensile strain allowable greater than about 1000×10^{-6} in./in. and a biaxial ultimate tensile stress allowable greater than about 500 psi. Because of the continuing stress relaxation, i.e. decreasing modulus with time, use of this stress criteria for computing seasonal thermal stress will then be conservative. The required strain allowable will not be conservative unless a suitable safety factor is used to account for unusual situations as well as for thermal fatigue.

6.3 Transient Thermal Distress

By considering the foundation to be rigid, and a transient thermal state of 20°F at the wearing surface and 70°F at the interface, from eq. 5.3b the strain as a function of depth into the pavement is

$$\epsilon(y) = (14 \times 10^{-6})(50)\left(1 - \frac{y^2}{H^2}\right) \quad (6.3a)$$

or 700×10^{-6} in./in. at the wearing course. If the change of ambient temperature occurred in 30 minutes,

$$E(t, T) = \left[2.5 \times 10^4\right] \left[\frac{1800}{(9.11 \times 10^5)(0.845^{20})}\right]^{-0.370} = 22 \times 10^4 \text{ psi} \quad (6.3b)$$

The stress is then

$$\sigma(t, T) = \frac{(22 \times 10^4)(700 \times 10^{-6})}{1 - 0.4} = 256 \text{ psi} \quad (6.3c)$$

The above calculations show that the stresses are considerably greater when the pavement is in thermal equilibrium compared to the transient state. Also, the stresses will be more severe for decreasing ambient temperatures than for increasing ambient temperatures. This is because of the fact that the pavement is continually relaxing. If the pavement is relaxed at some temperature and then the temperature decreases, tensile strains and stresses result. If

the pavement is in a relaxed state and then the temperature increases, compressive strains and stresses result. Since the tensile strength of bituminous concrete is considerably less than the compressive strength, decreasing temperatures cause the most damage.

6.4 Shear State at the Pavement-Foundation Interface

If the temperatures of the wearing course and the pavement-foundation interface are 70 and 20°F, respectively, the pavement is 4 in. thick, and the time is 30 minutes, the constants given by eq. 5.5 are

$$B = \frac{(2.5 \times 10^4)(1800)^{0.370} (14 \times 10^{-6})(50)}{(9.11 \times 10^5)^{-0.370} (0.845)^{-20(0.370)} (1-0.4)} = 87.5 \quad (6.4a)$$

and

$$b = 0.370(50) \ln(0.845) = -3.01 \quad (6.4b)$$

From eq. 5.6c, the shear force is

$$P = \frac{2(87.5)(4)}{3} + 2(87.5)(4) \sum_{n=1}^{\infty} \frac{(-3.01)^n}{n!(4n^2+5n+3)} = 130 \text{ lb} \quad (6.4c)$$

and the shear stress is then

$$\tau_f = \frac{2P}{W} = \frac{2 \times 130}{72} = 4 \text{ psi} \quad (6.4d)$$

The equations show that the shear stress increases in direct proportion to the thickness of lift. From strength of materials theory, the stresses in the wearing course and throughout the pavement thickness will increase severely if the interface has failed locally in shear. Further, since the transient state of parabolic temperature distribution was assumed in the development of the relations, the interface shear stress will be on the order of one and one-half times greater than that just calculated when the thermal equilibrium state is reached at low temperatures.

6.5 Debond by Peel Mechanism

If again the temperatures of the wearing course and the pavement-foundation interface are 70 and 20°F, respectively, the pavement is 4 in. thick, and the time is 30 minutes, the constants already computed can be used to calculate the peel moment; i.e. if $B = 87.5$ and $b = 3.01$, then the reference moment from eq. 5.8c is

$$\bar{m}(t, T) = \frac{87.5(4^2)}{4} + \frac{87.5(4^2)}{2} \sum_{n=1}^{\infty} \frac{(-3.01)^n}{n!(n^2+3n+2)} = 159 \text{ in.-lb.} \quad (6.4e)$$

The peel moment is therefore

$$m(t, T) = \frac{159}{3} = 53 \text{ in.-lb.} \quad (6.4f)$$

The peel moment is a maximum of 53 in.-lb at the pavement edge and decreases to a minimum at the lane centerline due to the pavement weight. The peel requirement is important because, as shown schematically in Fig. 24, once the pavement debonds, the propensity for loss of structural integrity due to mechanical loads becomes accentuated. An edge debond would allow the accumulation of a thin film of water, which by the pumping action of wheel loads would lead to a local foundation washout. Loss of localized foundation support would then result in an accelerated fatigue failure.

6.6 Implications of the Results

While this work was primarily concerned with thermal distress, and although the effects from mechanical loads and thermal loads might be considered separately in the analysis, the final design must consider the combined loading conditions. The principal components of the induced distress are:

a. The whole field mechanical stresses in the system due to wheel loads is analogous to a uniformly supported plate with a concentrated load. This loading gives flexural stresses which could be viewed as compressive at the top surface of the pavement and tensile at the bottom surface.

b. The local effects of stress concentration due to wheel load are tensile longitudinal stresses at the pavement surface and at the bottom surface, with the magnitude greater at the top surface.

c. The worst case of thermal distress is for decreasing transient ambient temperature. In this situation the thermal stresses at the surface and at the pavement-foundation interface are tensile, with the magnitude greater at the top surface.

Superposition of the preceding stresses shows that the thermal stress tends to decrease the stress due to mechanical load in the wearing course, whereas the thermal stress aggravates the mechanical stress at the pavement-foundation interface. This indicates that pavement cracks must often originate at the pavement-foundation interface and then propagate up through the wearing course, which is in contradistinction to a common assumption that pavement cracks always originate at the surface of the pavement.

CHAPTER VII

CONCLUSIONS AND RECOMMENDATIONS

7.1 Conclusions

1. Equations were developed for finding the thermoviscoelastic strains and stresses in the pavement for either isothermal conditions or transient temperature distributions.

2. The pavement will crack due to thermal changes alone if the material allowables are not greater than those calculated from the given equations. (See equations 4.10c, 4.13, 5.4b.)

3. Seasonal changes in temperature cause greater distress than transient changes.

4. Decreasing ambient temperatures are considerably more damaging to the pavement than increasing ambient temperatures.

5. Due to the shear lag the thermal distress is greater at the pavement-foundation interface than in the wearing course.

6. The thermal shear lag is significant in relatively thick pavements and negligible in thin lifts.

7. An equation (5.7b) was developed for determining the required thermoviscoelastic shear stress at the pavement-foundation interface. The allowable wheel load capacity of the pavement is reduced if the interface fails in shear, which will result in cracks being initiated at the interface.

8. An equation (5.9c) was developed for determining the required thermoviscoelastic peel strength. The loss of structural

integrity from the peel standpoint will lead to rapid deterioration of a flexible pavement with cracks being initiated at the surface course.

9. The combined distress due to wheel loads and thermal stress (or strain) is greater at the interface and smaller in the wearing course, compared to each effect taken singly, thereby causing most pavement cracks to originate at the interface and propagate upward through the wearing course.

7.2 Recommendations

1. It has been noted that the energy approach or classical methods provide insight concerning the relative importance of the various parameters when it is possible and feasible to use these methods. The finite element routines provide a method for more general analysis and it is recommended that a comprehensive thermo-viscoelastic master program be developed wherein the finite element technique is used in subroutines. Such a program could be conveniently used for parametric analysis of partially failed pavements, i.e. assessment of strain distributions of pavements containing hairline cracks.

2. Because of the problems associated with comparison of experimental results on asphaltic concrete, it is believed that material properties might be better defined in terms of a "standard mixture." A standard mixture may be defined as one composed of an aggregate of given size and grading and particles of uniform shape and surface texture

mixed with an adhesive binder of reasonable availability. The binder should possess what are considered to be desirable rheological properties and good resistance to hardening when exposed to environmental factors such as heat, air and solar radiation. The aggregate particles could be glass spheres, thereby eliminating variables in the mixture caused by particle shape, surface texture and chemical nature of the solid surface presented to the binder.

3. The solid propellant rocket motor industry has an extensive number of standard material property tests that are well proven and used routinely for quantitative evaluation. It is strongly recommended that these various standard tests (26) be used for determining the material properties of the standard mixture and real mixtures of asphaltic concrete.

4. To demonstrate the reduction of thermal stress by replacing some of the aggregate with crushed glass, it is suggested that model analogs in biaxial thermal stress be used to experimentally determine guidelines, followed by field implementation.

5. It is recommended that model analogs in biaxial thermal stress be used to demonstrate the feasibility of thermal strain relief by the use of sand-asphalt grid or plastic foam at the simulated pavement-foundation interface, followed by field implementation.

6. To show the efficiency of selective dewetting, it is recommended that the stresses and strains be determined in a centrally loaded, asphaltic concrete flexure beam where the outer layer on the tensile side has either a dewetting agent on the aggregate or

dirty aggregate, followed by field implementation.

7. It is recommended that models be constructed, using the beam analogy, to quantitatively assess the benefit of construction with plastic scrim in the wearing course. Using "standard mixtures," with and without scrim, the strain distributions could be accurately determined with the Moire method or the Sandman method (birefringent coating technique).

NOMENCLATURE

<u>Symbol</u>	<u>Variable</u>	<u>Typical Units</u>
A	area	in. ²
a _T	time-temperature shift factor	numeric
c	constant	--
d	displacement	in.
E	Young's modulus	psi
e	$\epsilon_x + \epsilon_y + \epsilon_z$	in./in.
F	function	--
G	modulus of rigidity, $\frac{E}{2(1+\mu)}$	psi
H	depth of flexible pavement	in.
M	total moment	in.-lb
m	shear moment	in.-lb
n	index	numeric
P	force	lb
p	pressure	psi
R	$\frac{E_p}{E_f}$	numeric
T	temperature	°F
\bar{T}	$T_L - T_u$	°F
t	time	sec
u, v, w,	displacements in x, y, z directions, respectively	in.
\bar{u}	generalized displacement	in.
V	volume	in. ³
W	half width of highway lane	in.

<u>Symbol</u>	<u>Variable</u>	<u>Typical Units</u>
x,y,z	generalized coordinates	in.
α	linear coefficient of thermal expansion	in./in.-°F
$\bar{\alpha}$	$\alpha_p - \alpha_f$	in./in/-°F
β	thermal constraint energy density	in.-lb/in. ³
γ	shear strain	rad
ΔT	temperature difference	°F
μ	Poisson's ratio	numeric
ξ	strain energy density	in.-lb/in. ³
$\bar{\xi}$	strain energy	in.-lb
\mathbb{P}	potential	in.-lb
ρ	density	pcf
σ	normal stress	psi
τ	shear stress	psi
η	thermal strain energy density	in.-lb/in. ³

Subscripts

p	pavement
f	foundation
t	top
s	shear lag
d	differential
u	upper
l	lower

Abbreviations

AAPT Association of Asphalt Paving Technologists
AASHO American Association of State Highway Officials
ASTM American Society for Testing and Materials
HRB Highway Research Board
ICRPG Interagency Chemical Rocket Propulsion Group
THD Texas Highway Department
TTI Texas Transportation Institute
WASHO Western Association of State Highway Officials

REFERENCES

1. A. Osborn, address to 6th Annual Creative Problem-Solving Inst., Univ., Buffalo, 1960; reprinted in S. J. Parnes and H. R. Harding, A Source Book for Creative Thinking, 1962, Scribner's Publ., N. Y., p 19-30.
2. R. L. Alexander, "Limits of Linear Viscoelastic Behavior of an Asphalt Concrete in Tension and Compression," Ph.D. Dissertation, June 1964, Univ. Calif., Berkeley.
3. Asphalt, V 19, N 4, Oct. 1967, p 2.
4. J. F. Hills, and D. Brien, "The Fracture of Bitumens and Asphalt Mixes by Temperature Induced Stresses," AAPT, 1966, p 292-309.
5. C. L. Monismith, G. A. Secor, and K. E. Secor, "Temperature Induced Stresses and Deformations in Asphalt Concrete," AAPT, V 34, 1965, p 248-285.
6. B. G. Hutchinson, and R. C. G. Haas, "A System Analysis of the Highway Pavement Design Process," Hwy. Res. Rec. No. 239, 1968, p 1-24.
7. H. E. Schweyer, and J. C. Busot, "A New Approach to Asphalt Rheology," HRB, Jan. 1969.
8. K. P. George, "Cracking in Pavements Influenced by Viscoelastic Properties of Soil-Cement," HRB, Jan. 1969.
9. Y. T. Chou, and H. G. Larew, "Stresses and Displacements in Viscoelastic Pavement Systems under a Moving Load," HRB, Jan. 1969.
10. K. O. Anderson, B. P. Shields, and J. M. Dacyszyn, "Cracking of Asphalt Pavements Due to Thermal Effects," AAPT, V 35, 1966, p 247-262.
11. E. Zube, "Cracking of Asphalt Concrete Pavements Associated with Absorptive Aggregates," AAPT, V 35, 1966, p 270-290.
12. A. V. Dodd, "Considerations in Revision of Army Climatic Criteria," Proc. IES, 1968.
13. "The WASHO Road Test; Part 2: Test Data, Analysis, Findings," Spec. Rep. 22, 1955, HRB.

14. W. M. Moore, "Exploratory Study of Moisture Migration in Naturally Occurring Swelling Clays Related to Vertical Movements of Pavements," Ph.D. Dissertation, May 1965, Texas A&M Univ.
15. C. W. Beagle, "Compaction of Deep Lift Bituminous Stabilized Base," AAPT, V 35, 1966, p 549-566.
16. R. Bright, B. Steed, J. Steele, and A. Justice, "The Effect of Viscosity of Asphalt Properties of Bituminous Wearing Surface Mixtures," AAPT, V 35, 1966, p 164-206.
17. B. F. Kallas, "Asphalt Pavement Temperature," Hwy. Res. Rec. No. 150, 1966, p 1-11.
18. A. W. Johnson, "Frost Action in Roads and Airfields," Spec. Rep. 1, 1952, HRB.
19. C. L. Monismith, K. F. Secor, and E. W. Blackmer, "Asphalt Mixture Behavior in Repeated Flexure," AAPT, V 30, 1961, p 188-222.
20. H. S. Papazian, and R. F. Baker, "Analysis of Fatigue Type Properties of Bituminous Concrete," AAPT, V 28, 1959, p 179-210.
21. M. Ekse, "The Influence of Varying Amounts of Filler on Flexure Strength and Temperature Susceptibility of Compacted Asphaltic Concrete Mixtures," AAPT V 29, 1960, p 141-151.
22. W. A. Dunlap, and L. E. Stark, "Deflection Tests on Texas Highways," Bul. 269, 1960, HRB.
23. E. J. Yoder, "Flexible Pavement Deflections - Methods of Analysis and Interpretation," AAPT, V 31, 1962, p 260-288.
24. R. N. Hveem, "Pavement Deflections and Fatigue Failure," Bul. 114, 1955, HRB.
25. F. N. Finn, "Flexible Pavement Behavior - Method of Measurement," AAPT, V 31, 1962, p 210-230.
26. ICRPG Solid Propellant Mechanical Behavior Manual, Publ. No. 21, Feb. 1968, Army-Navy-Air Force-NASA, Working Group on Mechanical Behavior, Chemical Propulsion Information Agency, John Hopkins Univ., Appl. Physics Lab., 8621 Georgia Ave, Silver Springs, Md.

